FLUORESCENCE FOUNDATION

Advanced Fluorescence Microscope Workshop
Urbana-Champaign, Illinois
August 17-20, 2015

David Jameson

Time-Resolved Fluorescence and FLIM

FIGURE 1.6 Painting of George Gabriel Stokes, 1891, by Hubert von Herkomer, from the Royal Society Collection. Downloaded on March 29, 2013 from: http://www.bbc.co.uk/arts/yourpaintings/paintings/george-stokes-18191903-216241/

Since the seminal paper by Stokes, which contained the first true understanding of the fluorescence phenomenon, there has been curiosity about the duration of fluorescence, i.e., the fluorescence lifetime.

XXX. *On the Change of Refrangibility of Light.* By G. G. Stokes, *M.A., F.R.S., Fellow of Pembroke College, and Lucasian Professor of Mathematics in the University of Cambridge.*

Received May 11,—Read May 27, 1852.

224. But by far the most striking point of contrast between the two phenomena, consists in the apparently instantaneous commencement and cessation of the illumination, in the case of internal dispersion, when the active light is admitted and cut off. There is nothing to create the least suspicion of any appreciable duration in the effect. When internal dispersion is exhibited by means of an electric spark, it appears no less momentary than the illumination of a landscape by a flash of lightning. I have not attempted to determine whether any appreciable duration could be made out by means of a revolving mirror.

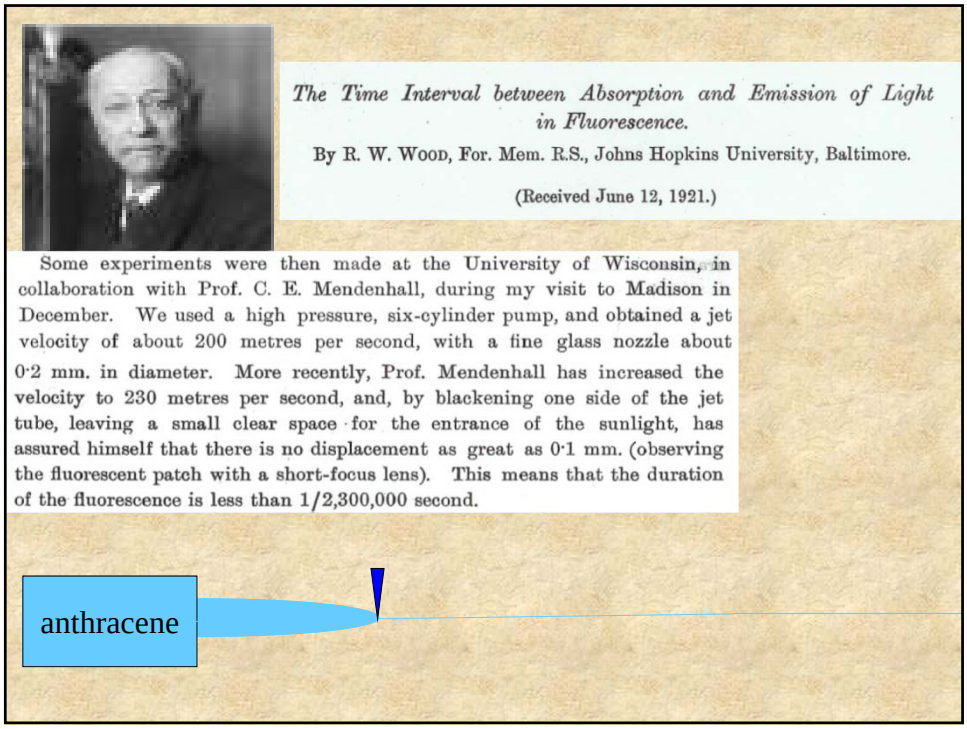
The Time Interval between Absorption and Emission of Light in Fluorescence.
By R. W. Wood, For. Mem. R.S., Johns Hopkins University, Baltimore.
(Received June 12, 1921.)
Some experiments were then made at the University of Wisconsin, in collaboration with Prof. C. E. Mendenhall, during my visit to Madison in December. We used a high pressure, six-cylinder pump, and obtained a jet velocity of about 200 metres per second, with a fine glass nozzle about 0·2 mm. in diameter. More recently, Prof. Mendenhall has increased the velocity to 230 metres per second, and, by blackening one side of the jet tube, leaving a small clear space for the entrance of the sunlight, has assured himself that there is no displacement as great as 0·1 mm. (observing the fluorescent patch with a short-focus lens). This means that the duration of the fluorescence is less than 1/2,300,000 second.
anthracene

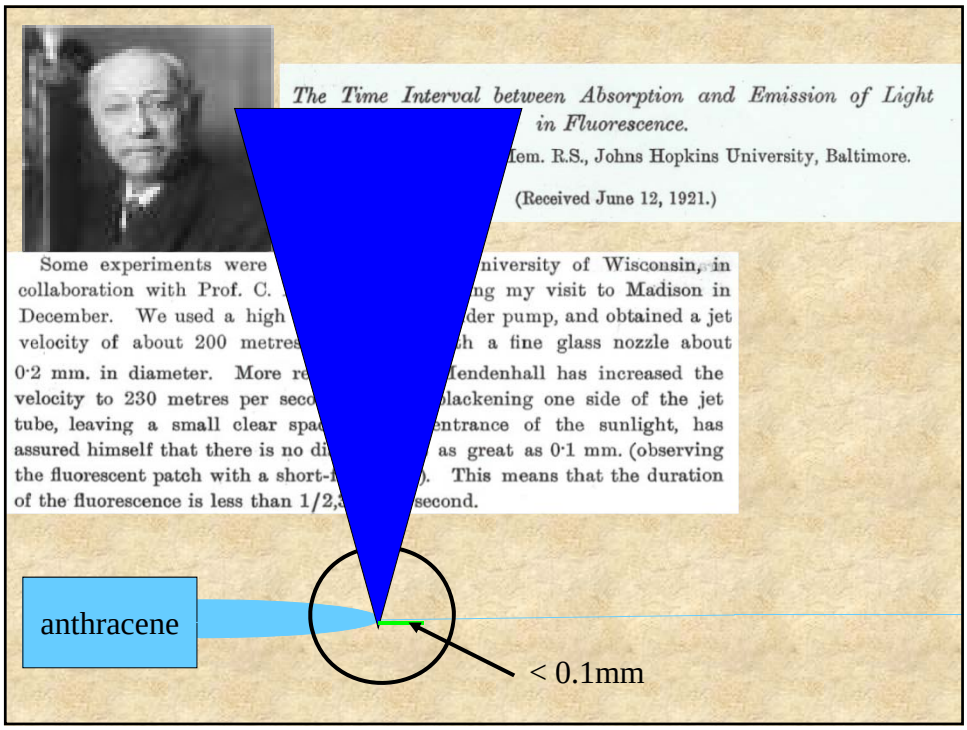
The Time Interval between Absorption and Emission of Light in Fluorescence.
(Received June 12, 1921.)
anthracene
< 0.1mm

The Time Interval between Absorption and Emission of Light in Fluorescence.

By R. W. Wood, For. Mem. R.S., Johns Hopkins University, Baltimore.

(Received June 12, 1921.)

Some experiments were then made at the University of Wisconsin, in collaboration with Prof. C. E. Mendenhall, during my visit to Madison in December. We used a high pressure, six-cylinder pump, and obtained a jet velocity of about 200 metres per second, with a fine glass nozzle about 0·2 mm. in diameter. More recently, Prof. Mendenhall has increased the velocity to 230 metres per second, and, by blackening one side of the jet tube, leaving a small clear space for the entrance of the sunlight, has assured himself that there is no displacement as great as 0·1 mm. (observing the fluorescent patch with a short-focus lens). This means that the duration of the fluorescence is less than 1/2,300,000 second.

i.e. < 435ns

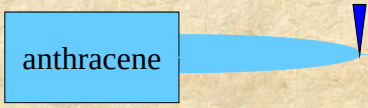

Enrique Gaviola

Ein Fluorometer.
Apparat zur Messung von Fluoreszenzabklingungszeiten.

Von E. Gaviola in Berlin.

Mit 9 Abbildungen. (Eingegangen am 24. März 1927.)

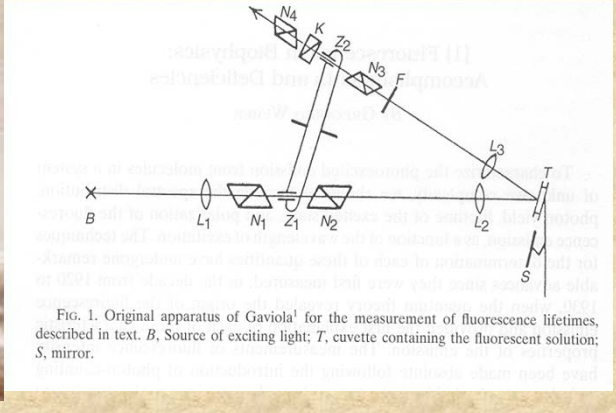

Fig. 1. Original apparatus of Gaviola[1] for the measurement of fluorescence lifetimes, described in text. *B*, Source of exciting light; *T*, cuvette containing the fluorescent solution; *S*, mirror.

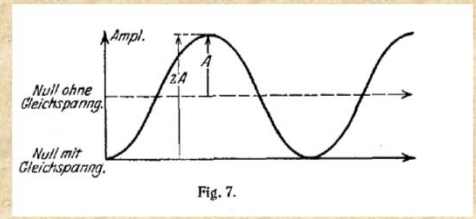

Fig. 7.

Farbstoff	Abklingungszeiten in Wasser Sekunden	in Glycerin Sekunden	in Meth.-Alkohol Sekunden
Uranin	$4{,}5 \cdot 10^{-9}$	$4{,}4 \cdot 10^{-9}$	—
Fluorescein	—	—	$5{,}0 \cdot 10^{-9}$
Rhodamin B	$2{,}0 \cdot 10^{-9}$	$4{,}2 \cdot 10^{-9}$	—
Rhodulin Orange	2,7	4,3	—
Erythrosin	1,8	2,4	$2{,}6 \cdot 10^{-9}$
Tetrajodfluor . Na	1,0	2,0	2,2
Eosin 5 B	1,9	—	3,4
Uranylsulfat	—	—	1,3
Uranylsulfat in Schwefelsäure	—	—	1,9
Chinisarin in Pentan	—	—	2,9
Uranglas	—	—	$>15{,}0$
Rubinkristall	—	—	$>15{,}0$

What is meant by the “lifetime” of a fluorophore???

Although we often speak of the properties of fluorophores as if they are studied in isolation, such is not usually the case.

Absorption and emission processes are almost always studied on *populations* of molecules and the properties of the supposed typical members of the population are deduced from the macroscopic properties of the process.

In general, the behavior of an excited population of fluorophores is described by a familiar rate equation:

$$\frac{dn^*}{dt} = -n^* \Gamma + f(t)$$

where n^* is the number of excited elements at time t, Γ is the rate constant of emission and f(t) is an arbitrary function of the time, describing the time course of the excitation . The dimensions of Γ are sec^{-1} (transitions per molecule per unit time).

If excitation occurs at t = 0, the last equation, takes the form:

$$\frac{dn^*}{dt} = -n^* \Gamma$$

and describes the decrease in excited molecules at all further times. Integration gives:

$$n^*(t) = n^*(0)\exp(-\Gamma t)$$

The lifetime, τ, is equal to Γ^{-1}

If a population of fluorophores are excited, the lifetime is the time it takes for the number of excited molecules to decay to 1/e or 36.8% of the original population according to:

$$\frac{n^*(t)}{n^*(0)} = e^{-t/\tau}$$

In pictorial form:

$$\frac{n^*(t)}{n^*(0)} = e^{-t/\tau}$$

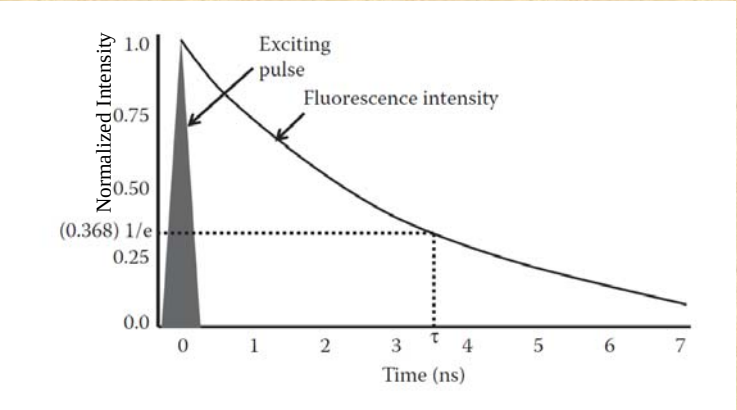

The lifetime and quantum yield for a given fluorophore is often dramatically affected by its environment.

Examples of this fact would be NADH, which in water has a lifetime of ~0.4 ns but bound to dehydrogenases can be a long as 9 ns.

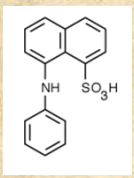

ANS in water is ~100 picoseconds but can be 15 – 20 ns bound to proteins

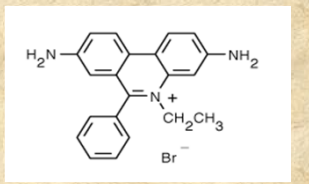

Ethidium bromide is 1.8 ns in water, 22 ns bound to DNA and 27ns bound to tRNA

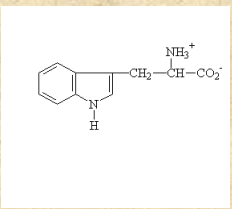

The lifetime of tryptophan in proteins ranges from ~0.1 ns up to ~8 ns

Excited state lifetimes have traditionally been measured using either the *impulse* response or the *harmonic* response method. In principle both methods have the same information content. These methods are also referred to as either the "time domain" method or the "frequency domain" method.

In the *impulse (*or pulse) method, the sample is illuminated with a short pulse of light and the intensity of the emission versus time is recorded. Originally these short light pulses were generated using *flashlamps* which had widths on the order of several nanoseconds. Modern laser sources can now routinely generate pulses with widths on the order of picoseconds or shorter.

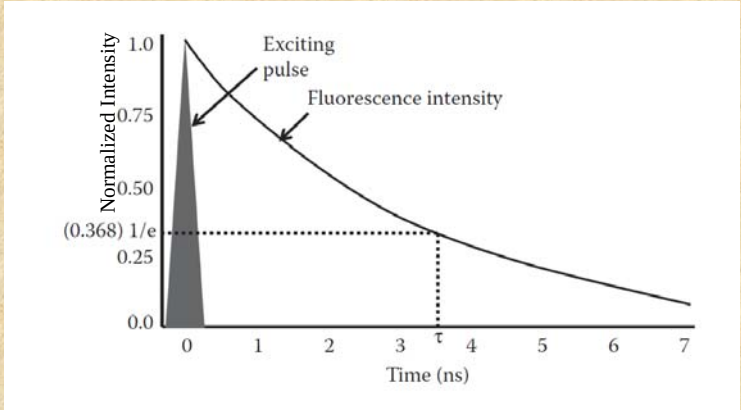

As shown in the intensity decay figure, the *fluorescence* lifetime, t , is the time at which the intensity has decayed to 1/e of the original value. The decay of the intensity with time is given by the relation:

$$I_t = \alpha e^{-t/\tau}$$

Where I_t is the intensity at time t, α is a normalization term (the pre-exponential factor) and τ is the lifetime.

It is more common to plot the fluorescence decay data using a logarithmic scale as shown here.

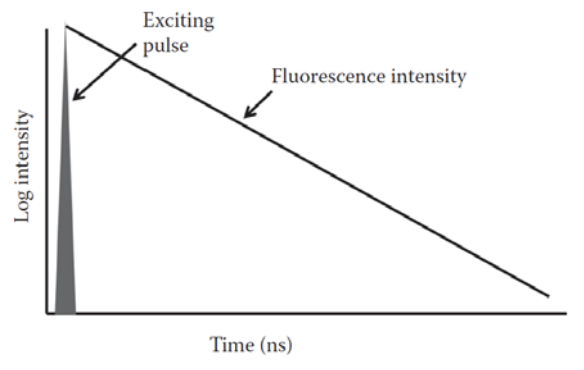

If the decay is a single exponential and if the lifetime is long compared to the exciting light then the lifetime can be determined directly from the slope of the curve.

If the lifetime and the excitation pulse width are comparable some type of *deconvolution* method must be used to extract the lifetime.

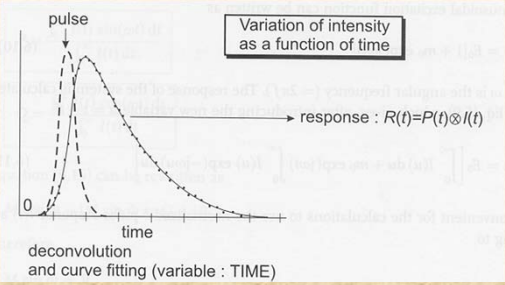

Great effort has been expended on developing mathematical methods to "deconvolve" the effect of the exciting pulse shape on the observed fluorescence decay.

With the advent of very fast laser pulses these deconvolution procedures became less important for most lifetime determinations, although they are still required whenever the lifetime is of comparable duration to the light pulse.

If the decay is multiexponential, the relation between the intensity and time after excitation is given by:

$$I(t) = \sum_i \alpha_i e^{-t/\tau_i}$$

One may then observe data such as those sketched below:

Here we can discern at least two lifetime components indicated as τ_1 and τ_2 . This presentation is oversimplified but illustrates the point.

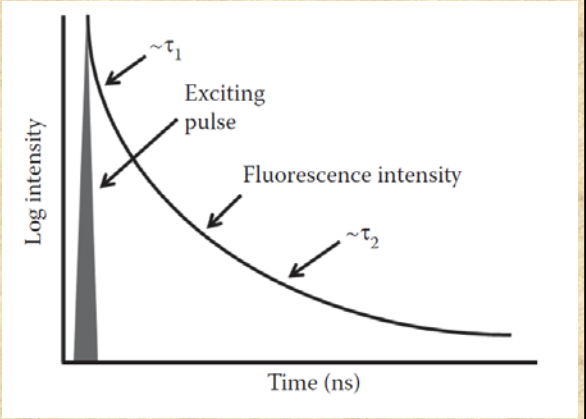

Here are pulse decay data on anthracene in cyclohexane taken on an IBH 5000U Time-correlated single photon counting instrument equipped with an LED short pulse diode excitation source.

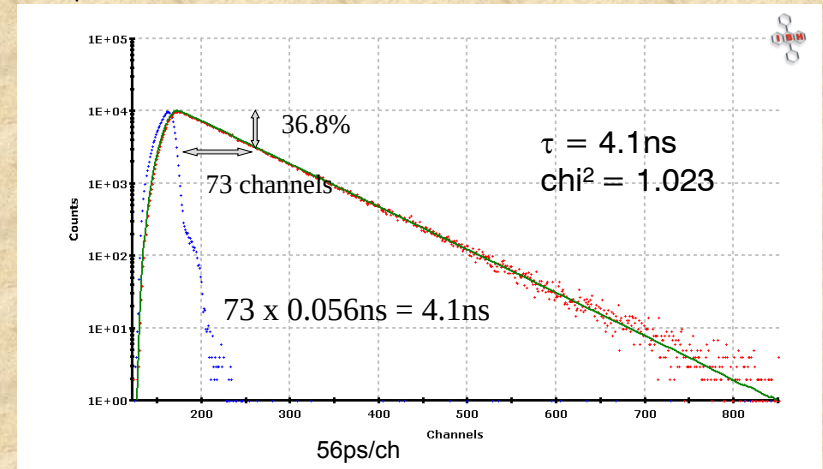

In the harmonic method (also known as the phase and modulation or frequency domain method) a continuous light source is utilized, such as a laser or xenon arc, and the intensity of this light source is modulated sinusoidally at high frequency as depicted below. Typically, an *electro-optic* device, such as a *Pockels cell* is used to modulate a continuous light source, such as a CW laser or a xenon arc lamp. Alternatively, LEDs or laser diodes can be directly modulated.

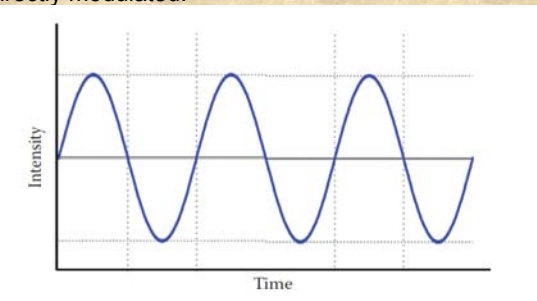

In such a case, the excitation frequency is described by:

$$E(t) = Eo\ [1 + M_E \sin \omega t]$$

E(t) and Eo are the intensities at time t and o, M_E is the modulation factor which is related to the ratio of the AC and DC parts of the signal and ω is the angular modulation frequency.
$\omega = 2\pi f$ where f is the linear modulation frequency

Due to the persistence of the excited state, fluorophores subjected to such an excitation will give rise to a modulated emission which is shifted in phase relative to the exciting light as depicted below.

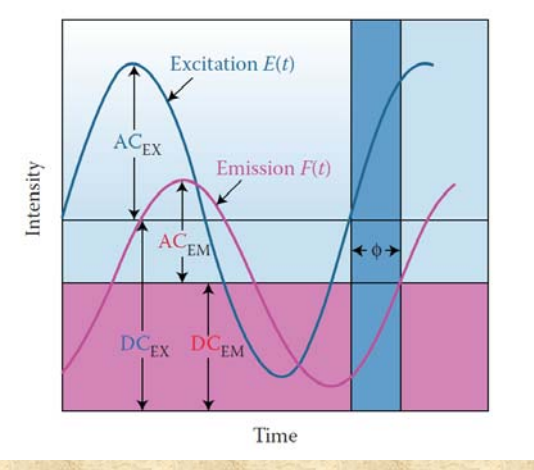

This sketch illustrates the phase delay (ϕ) between the excitation, E(t), and the emission, F(t). Also shown are the AC and DC levels associated with the excitation and emission waveforms.

One can demonstrate that:

$$F(t) = Fo\,[1 + M_F \sin(\omega t + \phi)]$$

This relationship signifies that measurement of the phase delay, ϕ, forms the basis of one measurement of the lifetime, τ. In particular one can demonstrate that:

$$\tan \phi = \omega\tau$$

The *modulations* of the excitation (M_E) and the emission (M_F) are given by:

$$M_E = \left(\frac{AC}{DC}\right)_E \quad \text{and} \quad M_F = \left(\frac{AC}{DC}\right)_F$$

The *relative modulation*, M, of the emission is then:

$$M = \frac{(AC/DC)_F}{(AC/DC)_E}$$

τ can also be determined from M according to the relation: $M = \dfrac{1}{\sqrt{1+(\omega\tau)^2}}$

Using the *phase shift* and *relative modulation* one can thus determine a *phase lifetime* (τ_P) and a *modulation lifetime* (τ_M).

If the fluorescence decay is a single exponential, then τ_P and τ_M will be equal at all modulation frequencies.

If, however, the fluorescence decay is multiexponential then $\tau_P < \tau_M$ and, moreover, the values of both τ_P and τ_M will depend upon the modulation frequency, i.e.,

$$\tau_P(\omega_1) < \tau_P(\omega_2) \quad \text{if} \quad \omega_1 > \omega_2$$

To get a feeling for typical phase and modulation data, consider the following data set.

Frequency (MHz)	τ_P (ns)	τ_M (ns)
5	6.76	10.24
10	6.02	9.70
30	3.17	6.87
70	1.93	4.27

These differences between τ_P and τ_M and their frequency dependence form the basis of the methods used to analyze for lifetime heterogeneity, i.e., the component lifetimes and amplitudes.

In the case just shown, the actual system being measured was a mixture of two fluorophores with lifetimes of 12.08 ns and 1.38 ns, with relative contributions to the total intensity of 53% and 47% respectively.

Here must must be careful to distinguish the term *fractional contribution to the total intensity* (usually designated as f) from α, the pre-exponential term referred to earlier. The relation between these two terms is given by:

$$f_i = \frac{\alpha_i \tau_i}{\sum_j \alpha_j \tau_j}$$

where j represents the sum of all components. In the case just given then, the ratio of the pre-exponential factors corresponding to the 12.08 ns and 1.38 ns components is approximately 1/8. In other words, there are eight times as many molecules in solution with the 1.38 ns lifetime as there are molecules with the 12.08 ns lifetime.

Multifrequency phase and modulation data are usually presented as shown below:

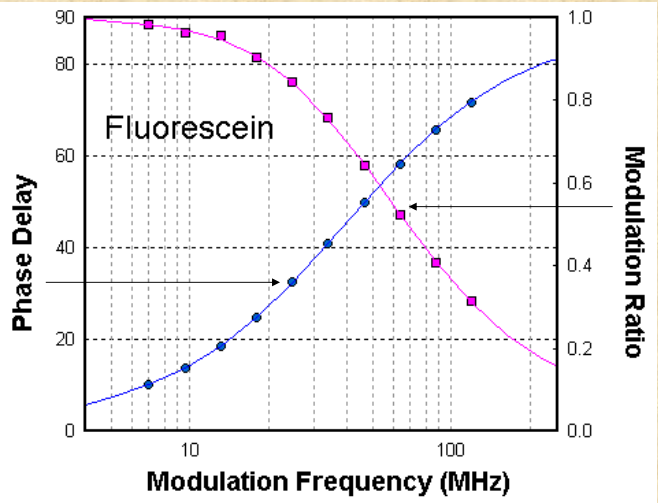

The plot shows the frequency response curve (phase and modulation) of Fluorescein in phosphate buffer pH 7.4 acquired on an ISS Chronos using a 470 nm LED. The emission was collected through a 530 high pass filter. The data is best fitted by a single exponential decay time of 4 ns.

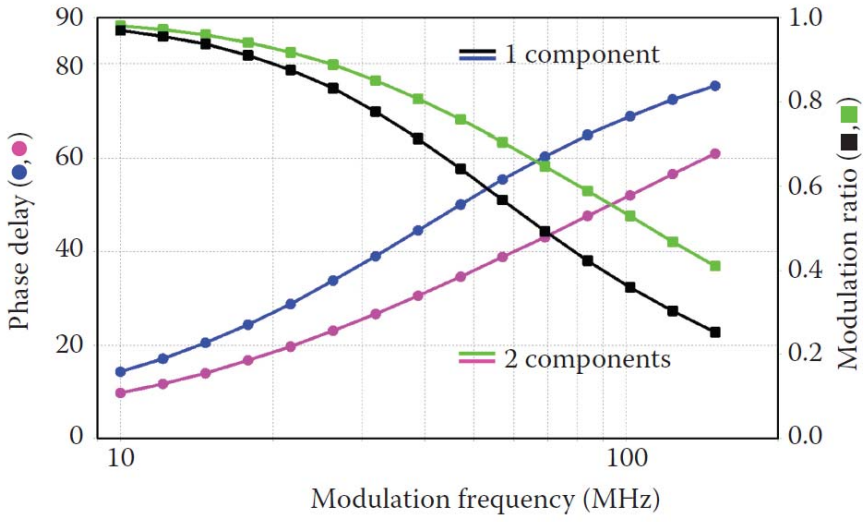

FIGURE 6.8 Simulation of phase and modulation data for a one-component system ($\tau = 4.05$ ns) and a two-component system ($\tau_1 = 4.05$ ns, $f_1 = 0.5$; $\tau_2 = 1.0$ ns, $f_2 = 0.5$). (I thank Carissa Vetromile for this figure.)

N. Boens, W. Qin, N. Basarić, J. Hofkens, M. Ameloot, J. Pouget, J.P. Lefèvre et al. 2007 Fluorescence lifetime standards for time and frequency domain fluorescence spectroscopy. *Anal Chem.* 79: 2137–2149.

Fluorophore	Solvent	FD Lifetime (ns)	TD Lifetime (ns)
Anthracene	MeOH	5.00	5.20
	Cyclohexane	5.32	5.32
9-Cyanoanthracene	MeOH	15.29	16.27
	Cyclohexane	12.39	13.47
9,10-Diphenylanthracene	MeOH	8.71	8.77
	Cyclohexane	7.17	7.76
N-methylcarbazole	Cyclohexane	14.06	14.15
Coumarin 153	MeOH	4.18	4.33
Erythrosine B	Water	0.090	0.089
	MeOH	0.45	0.48
NATA	Water	3.14	3.01
POPOP	Cyclohexane	1.12	1.12
PPO	MeOH	1.63	1.66
	Cyclohexane	1.35	1.38
Rhodamine B	Water	1.73	1.75
	MeOH	2.48	2.44
Rubrene	MeOH	9.79	9.97
N-(3-sulfopropyl) acridinium	Water	30.90	31.37
p-Terphenyl	MeOH	1.10	1.20
	Cyclohexane	0.96	1.00

In addition to decay analysis using discrete exponential decay models, one may also choose to fit the data to *distribution* models. In this case, it is assumed that the excited state decay characteristics of the emitting species actually results in a large number of lifetime components. Shown below is a typical lifetime distribution plot for the case of single tryptophan containing protein – human serum albumin.

The distribution shown here is Lorentzian but depending on the system different types of distributions, e.g., Gaussian or asymmetric distributions, may be utilized. This approach to lifetime analysis is described in: Alcala, J. R., E. Gratton and F. G. Prendergast. Fluorescence lifetime distributions in proteins. *Biophys. J. 51*, 597-604 (1987).

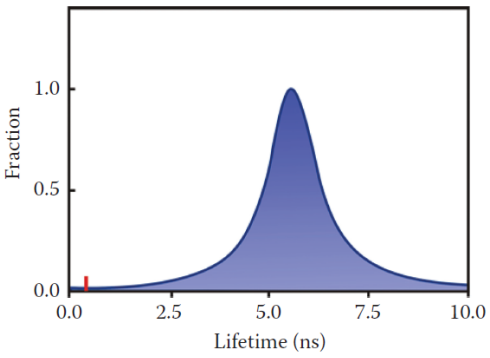

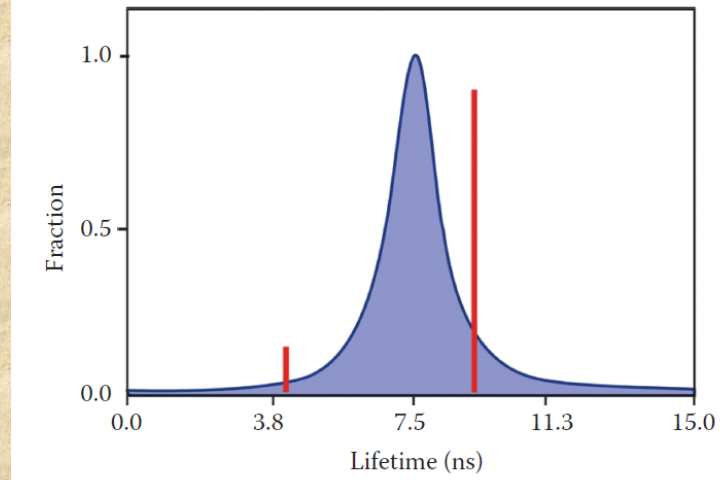

FIGURE 6.10 Comparison of discrete (red) and distribution (blue) lifetime analyses for mant-GDP bound to N-Ras protein P21. Both approaches give similar chi-square values. (Modified from D.M. Jameson and T.L. Hazlett 1991. *Biophysical and Biochemical Aspects of Fluorescence Spectroscopy*, pp. 105–133. Plenum Press, New York.)

Another popular lifetime analysis method – based on Information Theory - is the *Maximum Entropy Method* (MEM). In this method no *a priori* intensity decay model is assumed.

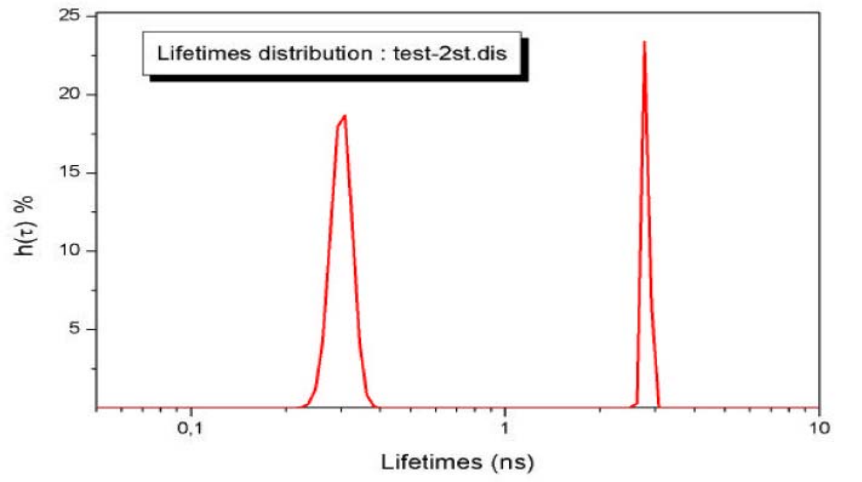

Jean-Claude Brochon
Maximum entropy method of data analysis in time-resolved spectroscopy. Methods Enzymol. 1994;240:262-311.

Global Analysis

In Global Analysis one can link decay parameters across many data sets which often allows for a more robust analysis

Example of the application of Global Analysis

Binding of Ethidium-Bromide to Transfer RNA

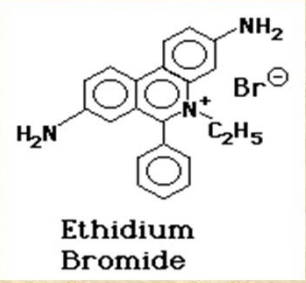

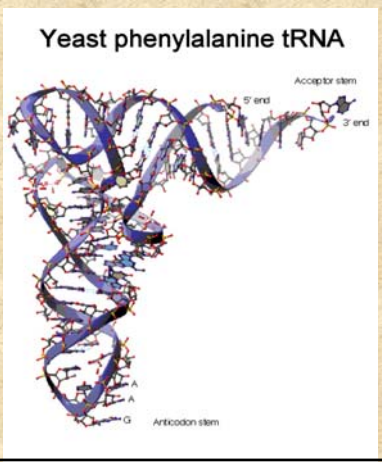

Ethidium bromide can intercalate into nucleic acid structures
It binds well to both DNA and RNA

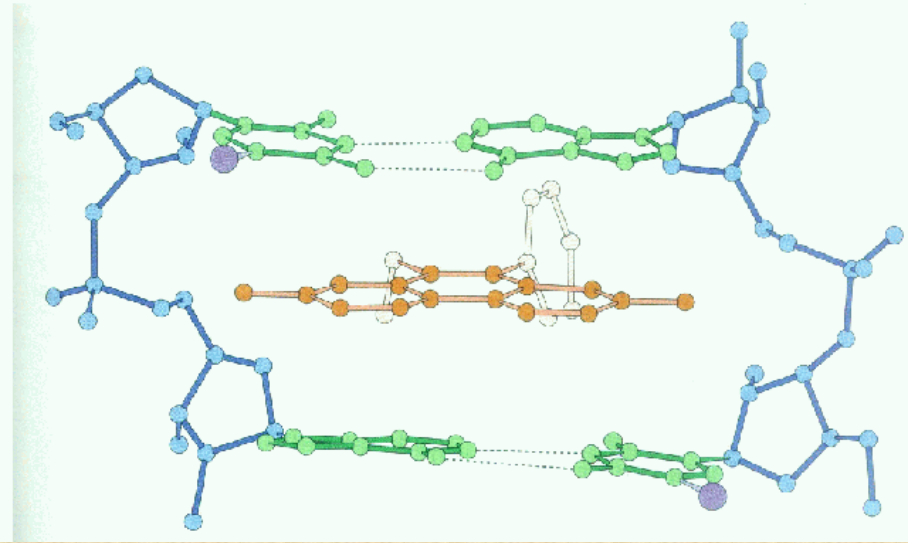

Fluorescence investigations of EB - tRNA interactions, carried out for more than 30 years, have indicated a "strong" binding site and one or more "weak, non-specific" binding sites.

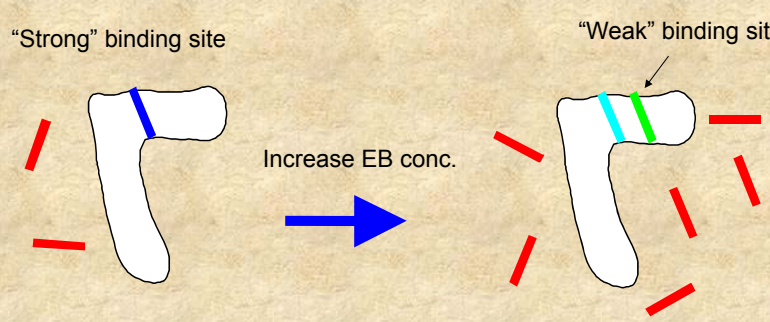

Question: What are the lifetimes of the strong and the weak binding sites???

If the tRNA is in excess only one EB will bind to the "strong" binding site which has a K_d of around 1 micromolar (under these conditions a single exponential decay of 27ns is observed). If the EB/tRNA ratio is increased, one or more additional EB's will bind and the question is: What are the lifetimes of EB bound to different sites on tRNA?" Shown below are phase and modulation data for a solution containing 124 μM yeast $tRNA^{phe}$ and 480 μM EB

The phase and modulation data were first fit to a single exponential component shown as the solid lines in the top plot. The residuals for this fit are shown in the bottom plot.

In this case τ = 18.49 ns and the χ^2 value was 250.

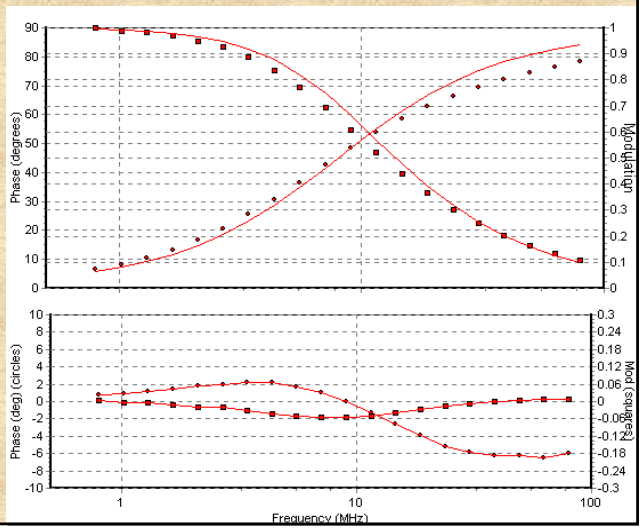

The data were then fit to a 2-component model shown here In this case the two lifetime components were 22.71 ns with a fractional intensity of 0.911 and 3.99 ns with a fractional intensity of 0.089.

The χ^2 for this fit was 3.06 (note the change in scale for the residual plot compared to the first case shown).

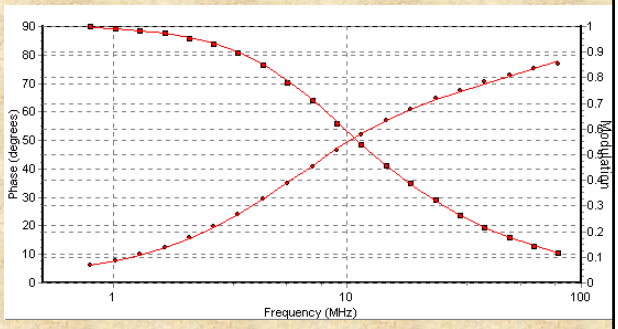

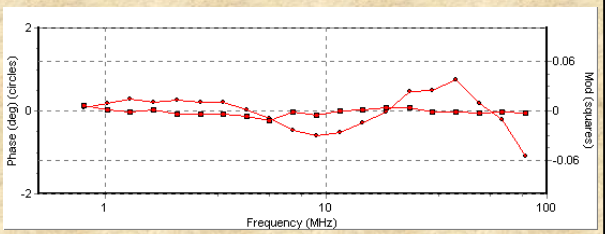

A 3-component model improves the fit still more. In this case

τ_1 = 24.25 ns, f_1 = 0.83

τ_2 = 8.79 ns, f_2 = 0.14

τ_3 = 2.09 ns, f_3 = 0.03

χ^2 = 0.39.

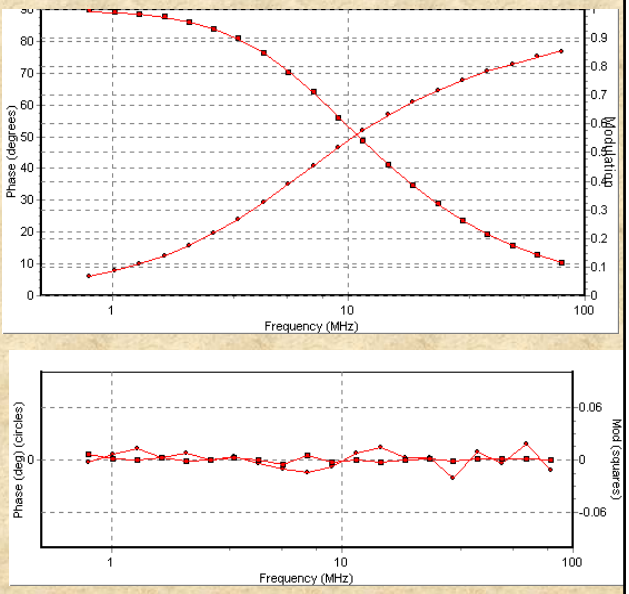

Adding a fourth component – with all parameters free to vary - does not lead to a significant improvement in the χ^2. In this case one finds 4 components of 24.80 ns (0.776), 12.13ns (0.163), 4.17 ns (0.53) and 0.88 ns (0.008).

But we are not using all of our information! We can actually fix some of the components in this case. We know that **free EB** has a lifetime of **1.84 ns** and we also know that the lifetime of **EB bound to the "strong" tRNA binding site** is **27 ns**. So we can fix these in the analysis. The results are four lifetime components of 27 ns (0.612), 18.33 ns (0.311), 5.85 ns (0.061) and 1.84 ns (0.016). The χ^2 improves to 0.16.

We can then go one step better and carry out **"Global Analysis"**.
In Global Analysis, multiple data sets are analyzed simultaneously and different parameters (such as lifetimes) can be "linked" across the data sets. The important concept in this particular experiment is that the lifetimes of the components stay the same and only their fractional contributions change as more ethidioum bromide binds.

In this system, 8 data sets, with increasing EB/tRNA ratios, were analyzed. Some of the data are shown below for EB/tRNA ratios of 0.27 (circles), 1.34 (squares), 2.41 (triangles) and 4.05 (inverted triangles).

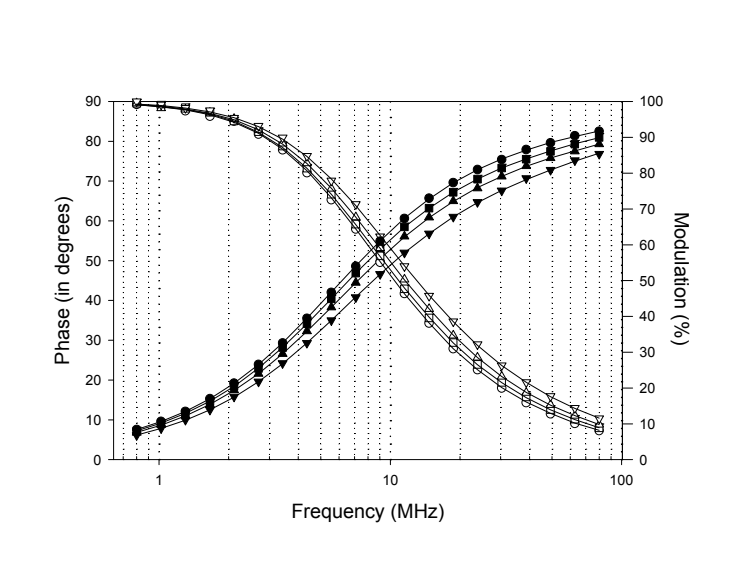

Global Analysis on seven data sets fit best to the 4 component model with two fixed components of 27ns and 1.84ns and two other components of 17.7ns and 5.4ns.

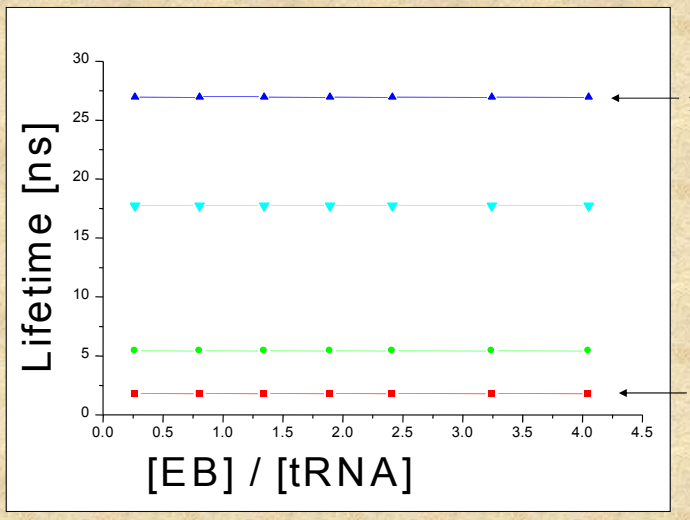

As shown in the plot below, as the EB/tRNA ratio increases the fractional contribution of the 27ns component decreases while the fractional contributions of the 17.7ns and 5.4ns components increase.

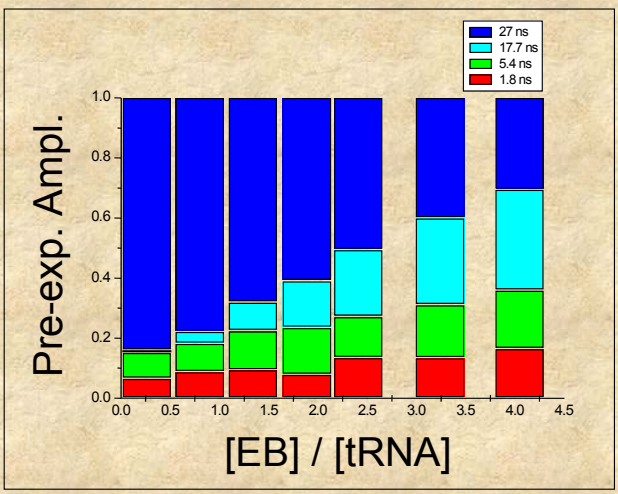

The Model

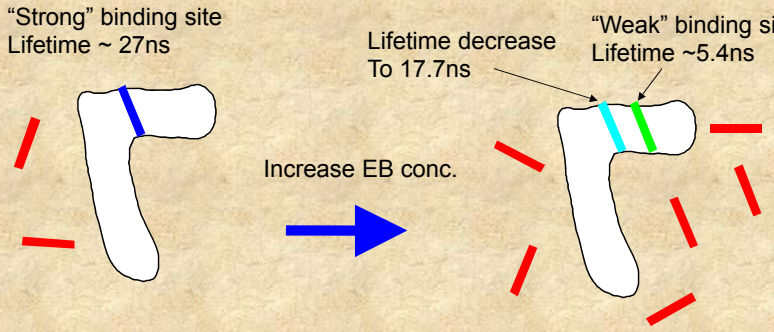

Question:
Is the drop in the lifetime of the "strong" binding site due to a change in tRNA conformation or energy transfer???

Answer: ???

Later in this workshop you'll learn about Fluorescence Lifetime Imaging or FLIM

In FLIM, lifetime data are obtained through a microscope - lifetime data is acquired at each pixel in the image

Lifetime data is more robust than intensity since it does not depend on how many fluorescent molecules are present

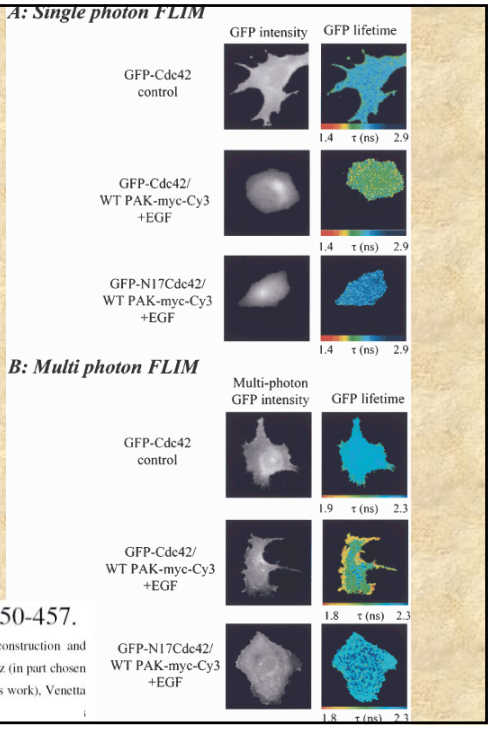

B. D. Venetta, *Rev. Sci. Instrum.*, 1959, **30**, 450-457.

In 1959 Venetta[74] described the construction and operation of a phase fluorometer coupled to a microscope. Using a frequency of 5.8 MHz (in part chosen due to the availability of FM transformers in televisions which could be salvaged for this work), Venetta was able to measure a lifetime of 2.7 ns for proflavin bound to the nuclei of tumor cells.

Why do FLIM?

FLIM is used for :

- **FRET**
- **Intracellular mapping of Ion concentration and pH imaging**
- **Biochemical reactions (oxidation/reduction) processes**
  - **NAD and NADH**
- **Long lifetime imaging (phosphorescence).**
  - **For example O_2 concentration in the cell or in tissues**

Also very useful to distinguish between desired signal and autofluorescence

Time Domain and Frequency Domain FLIM

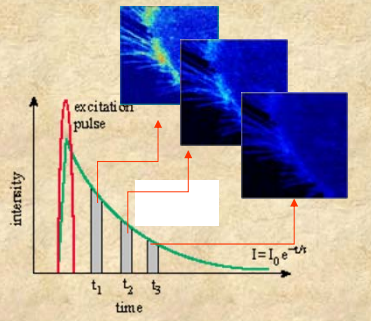

A sample is flashed many times by a short duration laser source

The histogram of the time intervals between the excitation flash, and 1st emitted photon is measured

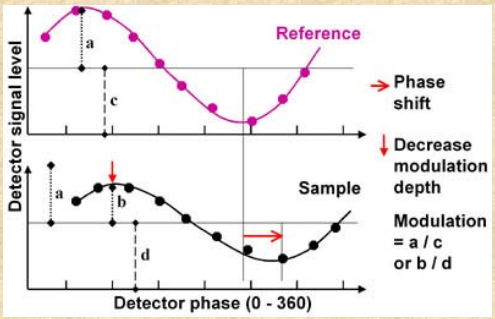

A sample is excited by a modulated light source

The fluorescence emission has the same frequency but is modulated and phase-shifted from the excitation source

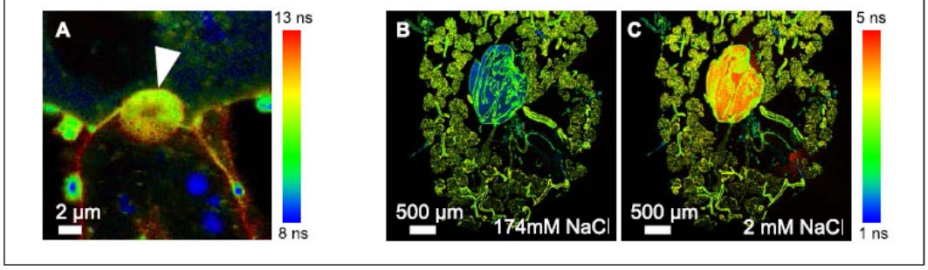

Fig. 2: Two examples for exploiting the fluorophore lifetime dependence on the local environment. A) Overview of HepG2 cells labeled with NBD tagged phosphlipids. The vacuole (marked with the white arrowhead) is enriched with fluorescent phospholipids. The lifetime difference to other compartments is clearly visible and provides information about the membrane structure. B) and C) Dissected salivary glands of an American cockroach, labeled with MQAE and placed in buffers with 174 mM NaCl (B) and 2 mM NaCl (C).Courtesy of Carsten Hille, Carsten Dosche, Potsdam University, Germany.

Fluorescence Lifetime Imaging (FLIM) in Confocal Microscopy Applications: An Overview

Susanne Trautmann, Volker Buschmann, Sandra Orthaus, Felix Koberling, Uwe Ortmann, Rainer Erdmann

PicoQuant GmbH, Rudower Chaussee 29, 12489 Berlin, Germany, info@picoquant.com

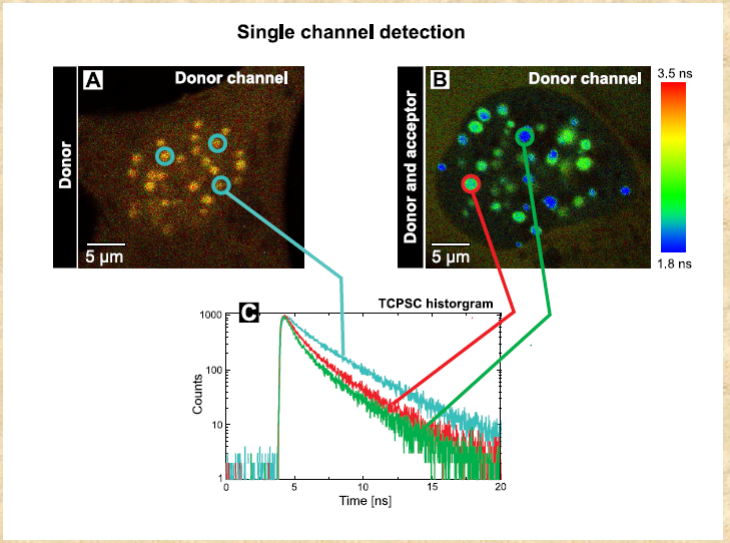

Picoquant

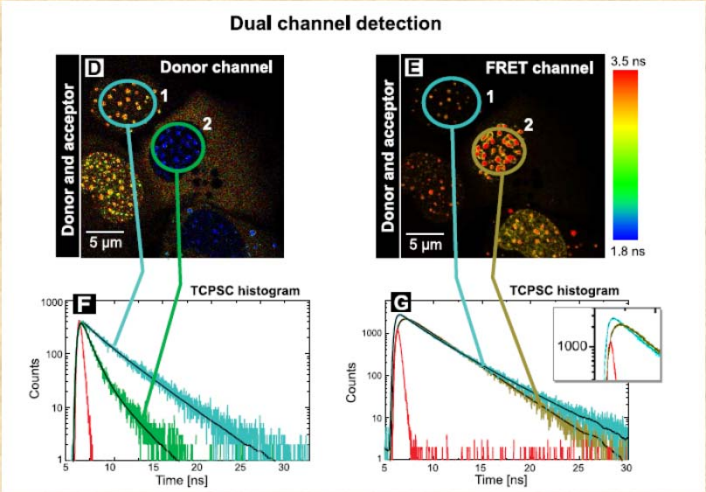

Picoquant

The challenges of FLIM

- At every pixel there are contributions of several fluorescent species, each one could be multi-exponential.
- To make things worse, we can only collect light for a limited amount of time (100-200 microseconds per pixel) which result in about 500-1000 photons per pixel.
- This is barely enough to distinguish a double exponential from a single exponential decay.
- Resolving the decay at each pixel in multiple components involves fitting to a function, and is traditionally a complex computational task "for experts only".

A major problem is **data analysis and interpretation**

A new approach: no more fits!

We propose a change in paradigm: Use a different representation of the decay where each molecular species has its own unique representation and where each process (FRET, ion concentration changes) is easily identified.

We need to go to a new "space"

Phasor space!!

Note – this is Enrico's joke – not mine!

Features of the phasor approach

Many of the obstacles in FLIM data analysis can be removed.
The accuracy of lifetime determination is improved

The speed of data analysis is reduced to almost instantaneous for an entire image or several images

The analysis is "global" over the image and across images.

The interpretation of the FLIM experiment is straightforward. Minimal prior spectroscopy knowledge is needed

The Phasor analysis method can be applied to all modes of data acquisition (frequency-domain and time-domain)

Ion concentrations can be calculated

Introduction to Phasors

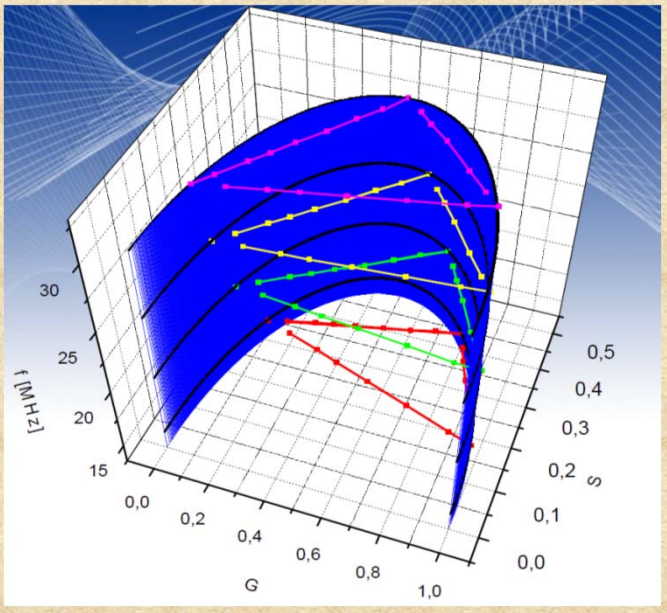

The phasor approach was dormant for many years until several laboratories began to apply it to FLIM

Tom Jovin
Andrew Clayton
Quentin Hanley ⇨ AB plots

Bob Clegg ⇨ polar plots

Enrico Gratton ⇨ phasor plots

More recently phasors have been applied to cuvette studies

Stefl, M., James, N.G., Ross, J.A. and Jameson, D.M. (2011) Anal. Biochem. 410:62-69. Application of Phasor to In Vitro Time-Resolved Fluorescence Measurements.

James, N.G., Ross, J.A., Stefl, M. and Jameson, D.M. (2011) Anal. Biochem. 410:70-76. Application of Phasor Plots to In Vitro Protein Studies.

Buscaglia, R., Jameson, D.M. and Chaires, J.B. (2012) Nucleic Acids Res. 40:4203-4215. G-Quadruplex structure and stability illuminated by 2-aminopurine phasor plots.

APPLIED SPECTROSCOPY REVIEWS, 20(1), 55-106 (1984)

The Measurement and Analysis of Heterogeneous Emissions by Multifrequency Phase and Modulation Fluorometry

DAVID M. JAMESON
Department of Pharmacology
The University of Texas Health Science Center at Dallas
Dallas, Texas 75235

ENRICO GRATTON
Department of Physics
University of Illinois at Urbana-Champaign
Urbana, Illinois 61801

ROBERT D. HALL
Laboratory of Molecular Biophysics
National Institute of Environmental Health Sciences
Research Triangle Park
North Carolina 27709

APPENDIX 2. PHASE AND MODULATION LIFETIME RELATIONS

We have asserted that a heterogeneous emitting population, in the absence of excited state reaction, will demonstrate a phase lifetime which is always less than the modulation lifetime. The algebraic demonstration of this fact is somewhat cumbersome [11, 68]. We present here a brief and more intuitive demonstration of the phenomenon.

One may make a simple geometrical representation of the phase delay and relative modulation as shown in Fig. 11. Here we depict a vector of length M making an angle ϕ with the x-axis where ϕ represents the phase delay and M the relative modulation. Since for a single exponential decay we have the relation $M = \cos \phi$, the endpoint of the vector is constrained to be on the circle of radius 1/2 with a center at (1/2, 0). The intercept of the extension of this vector with the line through x = 1 equals ωt (since $\tan \phi = \omega t$). This circle is universal for single exponential systems irrespective of the lifetime or modulation frequency. We note that the X and Y intercepts of the vector correspond to our previously defined G and S functions (since $G = M \cos \phi$ and $S = M \sin \phi$).

Figure 12 represents the case of two exponential decays with phase delays and relative modulations of ϕ_1, ϕ_2 and M_1, M_2, respectively. These decays contribute to the total emission intensity decay with fractional weights of f_1 and f_2, respectively. The total fluorescence observed is represented by the vector sum, M, of the two components and gives an observed phase delay of ϕ. Again we see that the intercept of the extension of the M vector with the x = 1 line corresponds to $\omega\tau^P$ (since $\tan \phi = \omega\tau^P$). The value of $\omega\tau^M$, however, corresponds to the line segment BD. This observation follows from the fact that the triangle OAB,

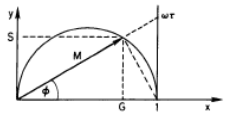

FIG. 11. Geometrical representation of phase delay (ϕ) and modulation ratio (M) for a single exponential decay.

Resolution of the Fluorescence Lifetimes in a Heterogeneous System by Phase and Modulation Measurements

Gregorio Weber

Department of Biochemistry, School of Chemical Sciences, University of Illinois, Urbana, Illinois 61801 (Received: August 12, 1980)

A closed-form procedure is described for the determination of the decay constants and the relative contributing intensities of the N independent components of a heterogeneous fluorescence emission employing measurements of the phase shift and relative modulation of the total fluorescence at N appropriate harmonic excitation frequencies. At each frequency the phase and modulation measurements yield the real part of the Fourier transform of the fluorescence impulse response, G, and its imaginary part, S. It is shown that the moments of a distribution of the lifetimes are linear combinations of the Gs (zero and even moments) or the Ss (odd moments), and the rule for the construction of the coefficients of G and S in these linear combinations is derived. The classical de Prony method is used to obtain the lifetimes and fractional contributions of the components from the moments. For binary and ternary mixtures the numerical computations required are trivial. In the present state of the art, the lifetimes of the components of a binary mixture should be derivable with a loss in precision somewhat smaller than 1 order of magnitude with respect to the overall measured lifetimes.

$$G_r = M_r \cos \Phi_r = [(1 + (\omega_r\tau_r^P)^2)(1 + (\omega_r\tau_r^M)^2)]^{-1/2} \quad (9)$$

$$S_r = M_r \sin \Phi_r = G_r\omega_r\tau_r^P \quad (10)$$

Frequency domain

$$G(\omega) = \int_0^\infty I(t) \cos \omega t \, dt$$

$$S(\omega) = -\int_0^\infty I(t) \sin \omega t \, dt \quad (55)$$

Time domain

APPLIED SPECTROSCOPY REVIEWS, 20(1), 55-106 (1984)

The Measurement and Analysis of Heterogeneous Emissions by Multifrequency Phase and Modulation Fluorometry

DAVID M. JAMESON
Department of Pharmacology
The University of Texas Health Science Center at Dallas
Dallas, Texas 75235

ENRICO GRATTON
Department of Physics
University of Illinois at Urbana-Champaign
Urbana, Illinois 61801

ROBERT D. HALL
Laboratory of Molecular Biophysics
National Institute of Environmental Health Sciences
Research Triangle Park
North Carolina 27709

APPENDIX 2. PHASE AND MODULATION LIFETIME RELATIONS

We have asserted that a heterogeneous emitting population, in the absence of excited state reaction, will demonstrate a phase lifetime which is always less than the modulation lifetime. The algebraic demonstration of this fact is somewhat cumbersome [11, 68]. We present here a brief and more intuitive demonstration of the phenomenon.

One may make a simple geometrical representation of the phase delay and relative modulation as shown in Fig. 11. Here we depict a vector of length M making an angle ϕ with the x-axis where ϕ represents the phase delay and M the relative modulation. Since for a single exponential decay we have the relation $M = \cos \phi$, the endpoint of the vector is constrained to be on the circle of radius 1/2 with a center at (1/2, 0). The intercept of the extension of this vector with the line through x = 1 equals ωt (since $\tan \phi = \omega t$). This circle is universal for single exponential systems irrespective of the lifetime or modulation frequency. We note that the X and Y intercepts of the vector correspond to our previously defined G and S functions (since $G = M \cos \phi$ and $S = M \sin \phi$).

Figure 12 represents the case of two exponential decays with phase delays and relative modulations of ϕ_1, ϕ_2 and M_1, M_2, respectively. These decays contribute to the total emission intensity decay with fractional weights of f_1 and f_2, respectively. The total fluorescence observed is represented by the vector sum, M, of the two components and gives an observed phase delay of ϕ. Again we see that the intercept of the extension of the M vector with the x = 1 line corresponds to $\omega\tau^P$ (since $\tan \phi = \omega\tau^P$). The value of $\omega\tau^M$, however, corresponds to the line segment BD. This observation follows from the fact that the triangle OAB,

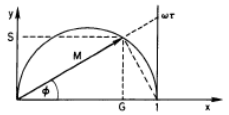

FIG. 11. Geometrical representation of phase delay (ϕ) and modulation ratio (M) for a single exponential decay.

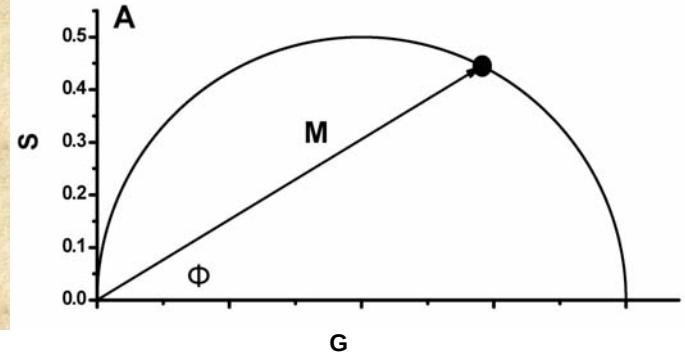

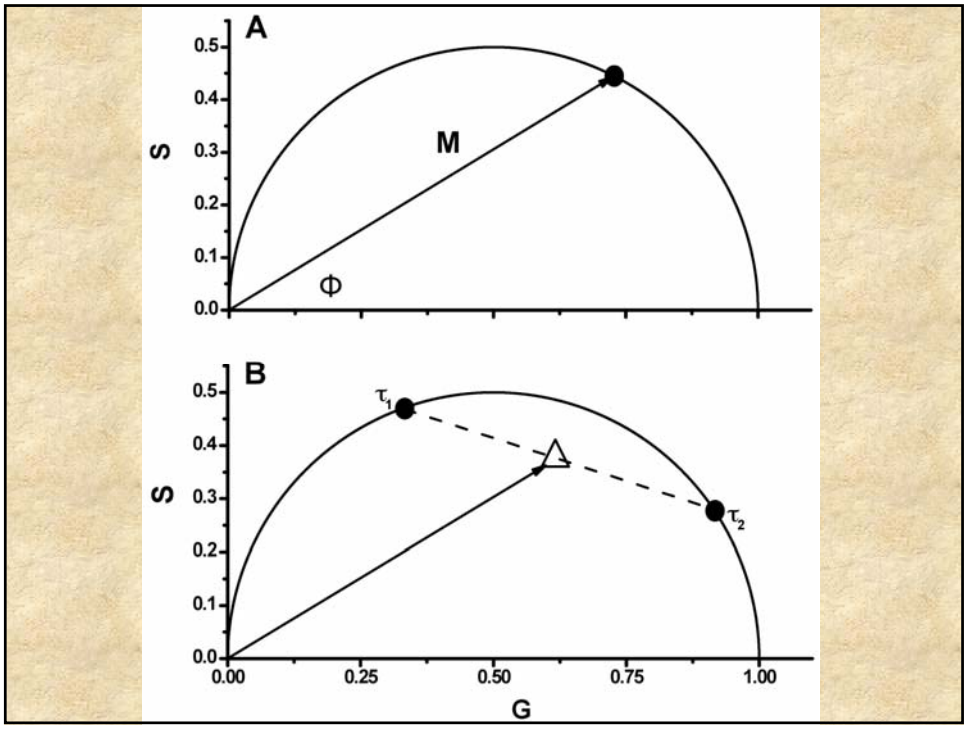

The algebra of phasors

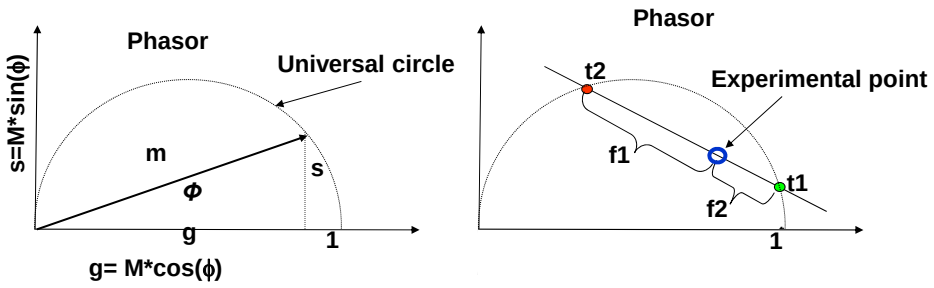

Simple rules to the Phasor plot:

1) All single exponential lifetimes lie on the “universal circle”
2) Multi-exponential lifetimes are a linear combination of their components
3) The ratio of the linear combination determines the fraction of the components

Slide from Enrico

Journal of Fluorescence, Vol. 1, No. 3, 1991

A Method for On-Line Background Subtraction in Frequency Domain Fluorometry

Gregory D. Reinhart,[1,2] Pasquina Marzola,[3] David M. Jameson,[2,4] and Enrico Gratton[5,6]

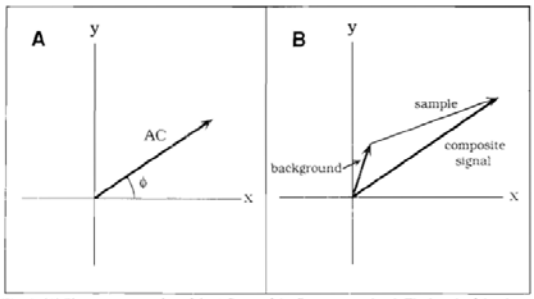

Fig. 1. (A) Phasor representation of the AC part of the fluorescence signal. The length of the phasor is proportional to the AC value, and the angle is equal to the phase angle as indicated. (B) Vector composition of background and sample signal to give the overall measured signal.

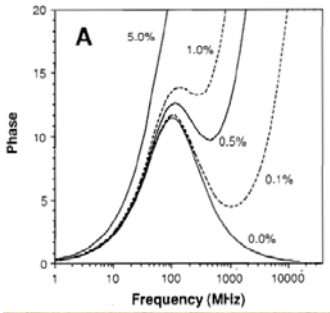

Methodological measurements I

- Map the position of the mixture of three different single-exponential dyes (Rhodamine B, AEDANS, DENS)

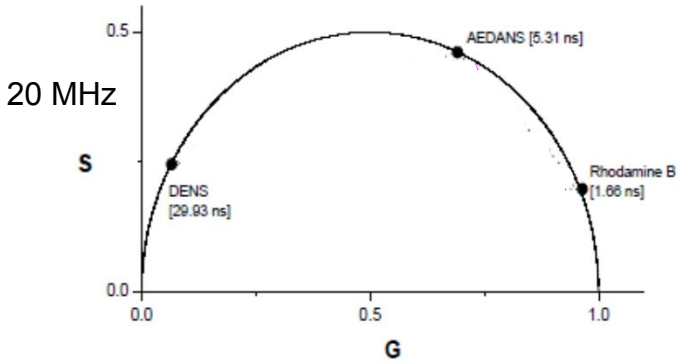

Methodological measurements I

- Map the position of the mixture of three different single-exponential dyes (Rhodamine B, AEDANS, DENS)
- The mixture lies inside the hypothetical triangle
- When some of the dye is added to the mixture – the point is moved towards the appropriate triangle vertex

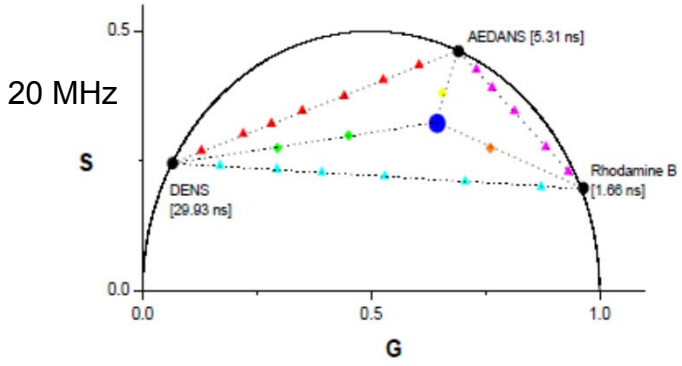

Methodological measurements II

- When analyzed for different frequencies – position of the hypothetical triangle in universal circle is anticlockwisely shifted when modulation frequency is increased
- Middle points copy the curvature of the universal circle

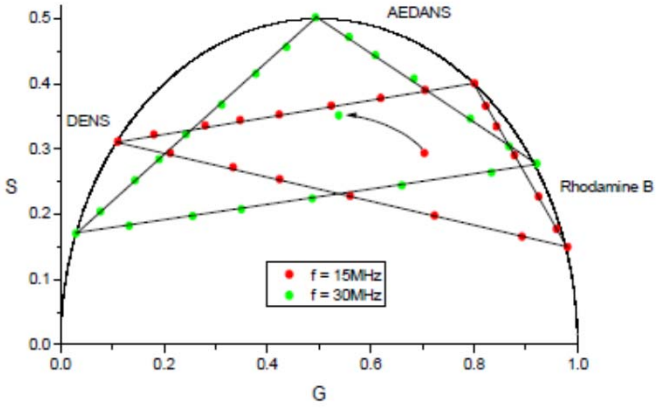

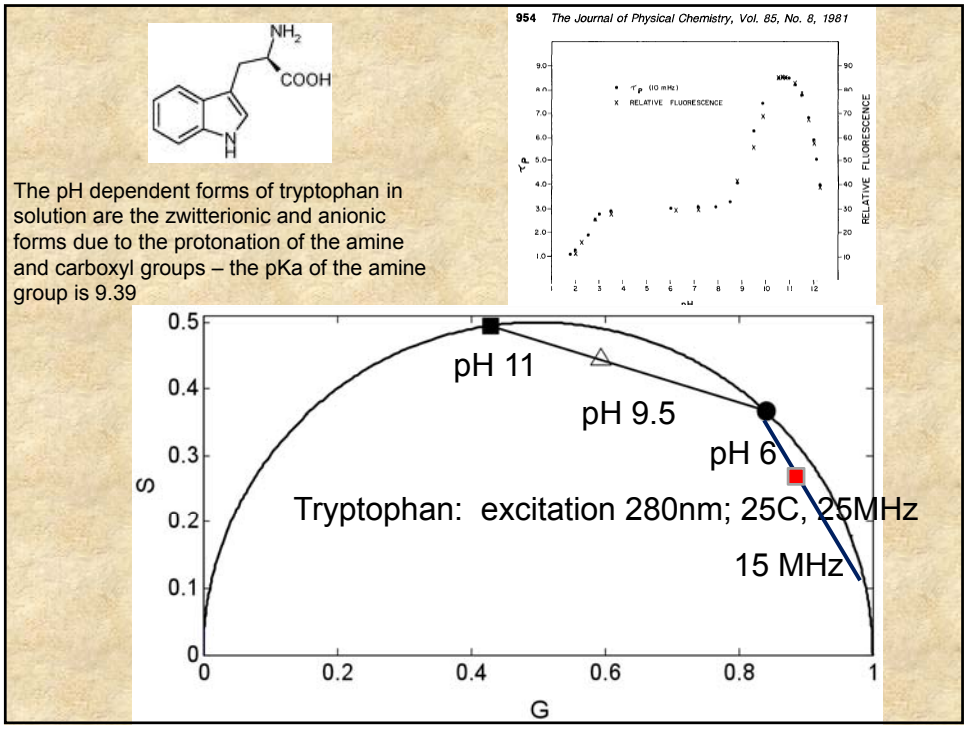
NH2
COOH
The pH dependent forms of tryptophan in solution are the zwitterionic and anionic forms due to the protonation of the amine and carboxyl groups – the pKa of the amine group is 9.39
954 The Journal of Physical Chemistry, Vol. 85, No. 8, 1981
RELATIVE FLUORESCENCE
pH 11
pH 9.5
pH 6
Tryptophan: excitation 280nm; 25C, 25MHz
15 MHz
S
G

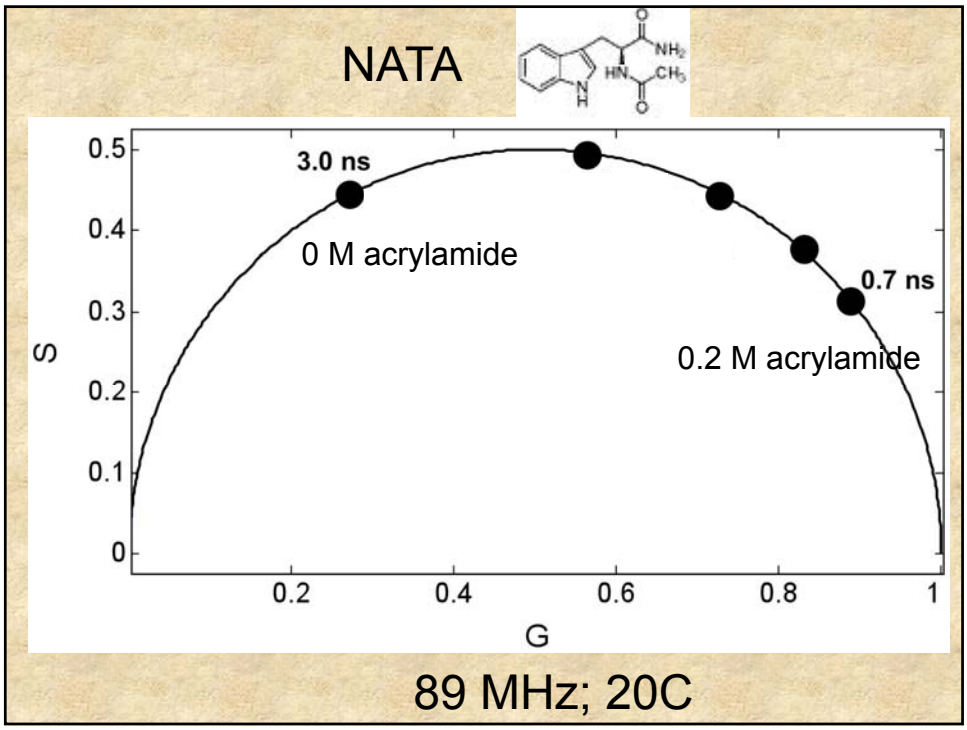
NATA
3.0 ns
0 M acrylamide
0.7 ns
0.2 M acrylamide
S
G
89 MHz; 20C

lysozyme

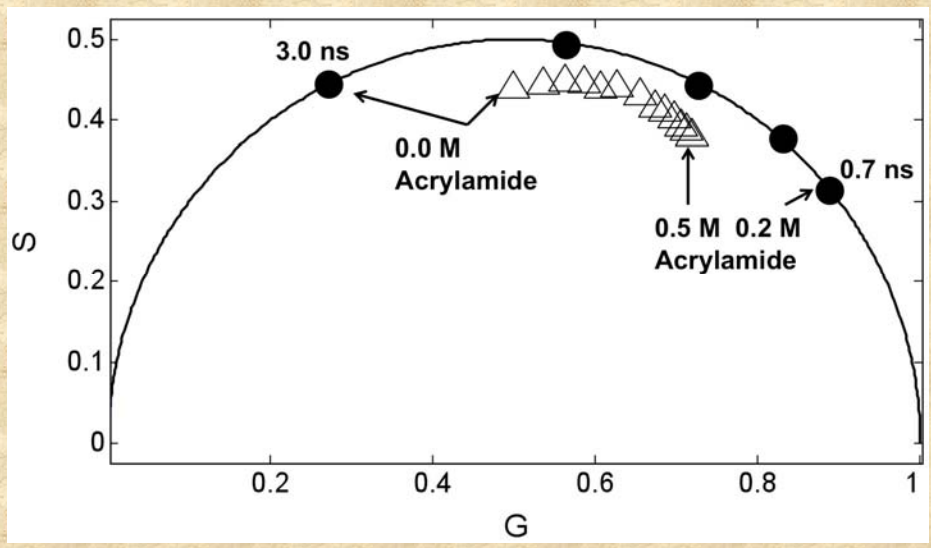

89 MHz; 20C

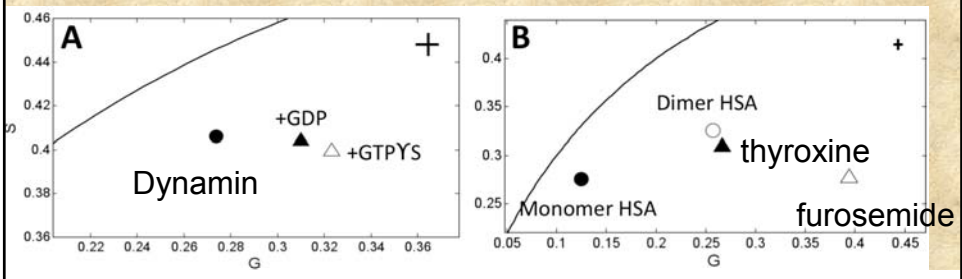

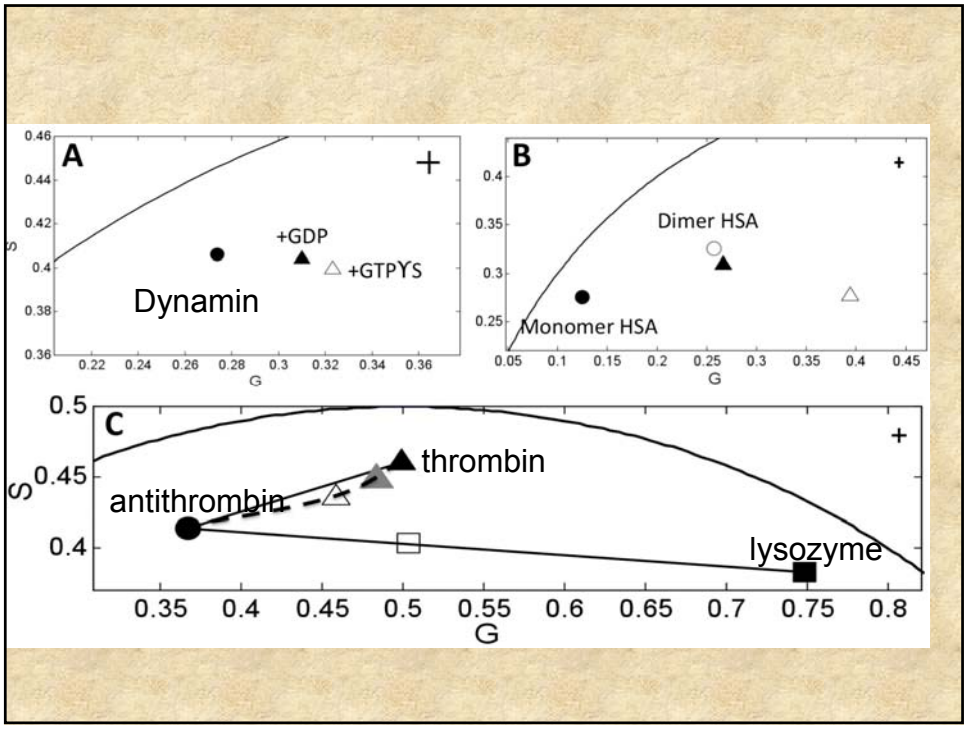
A
+GDP
+GTPγS
Dynamin
B
Dimer HSA
Monomer HSA
C
thrombin
antithrombin
lysozyme
S
G

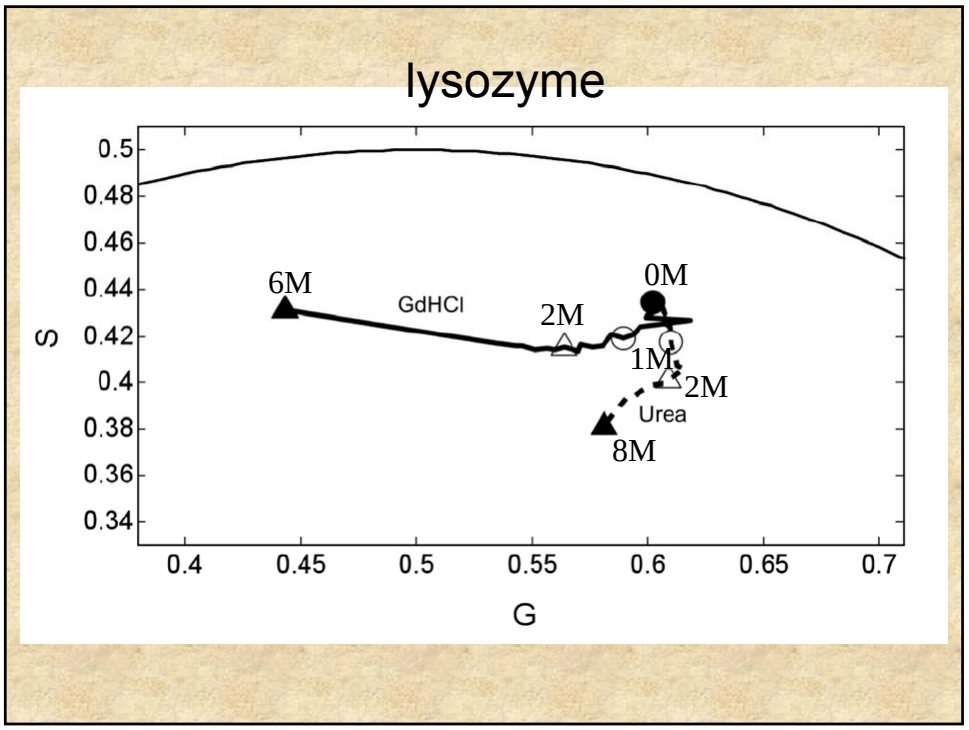
lysozyme
6M
GdHCl
2M
0M
1M
2M
Urea
8M
S
G

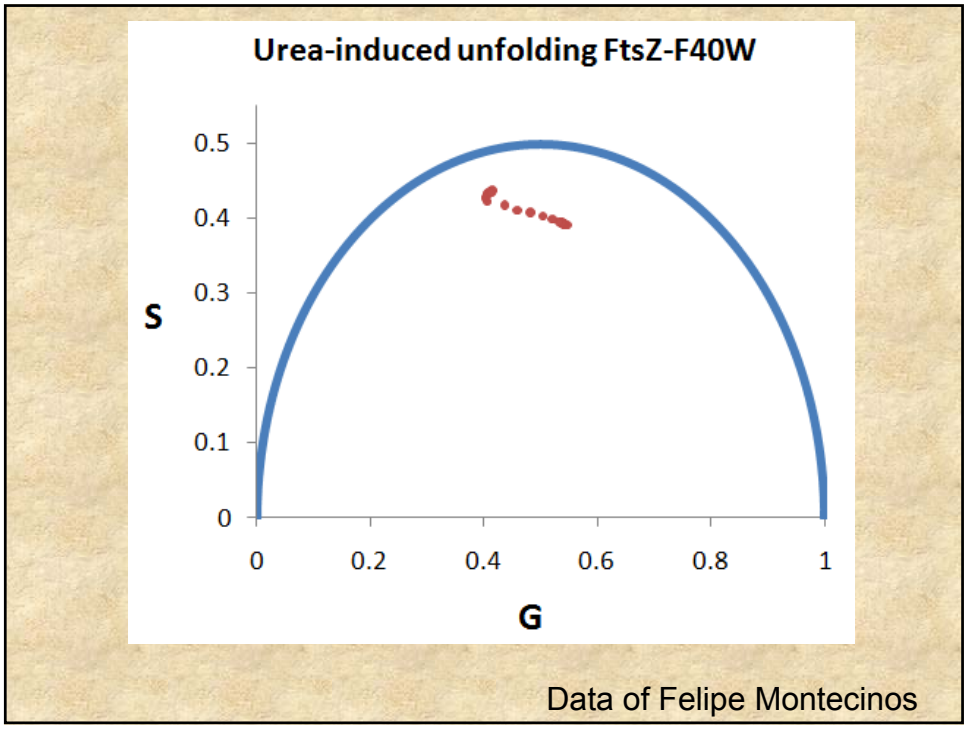

Data of Felipe Montecinos

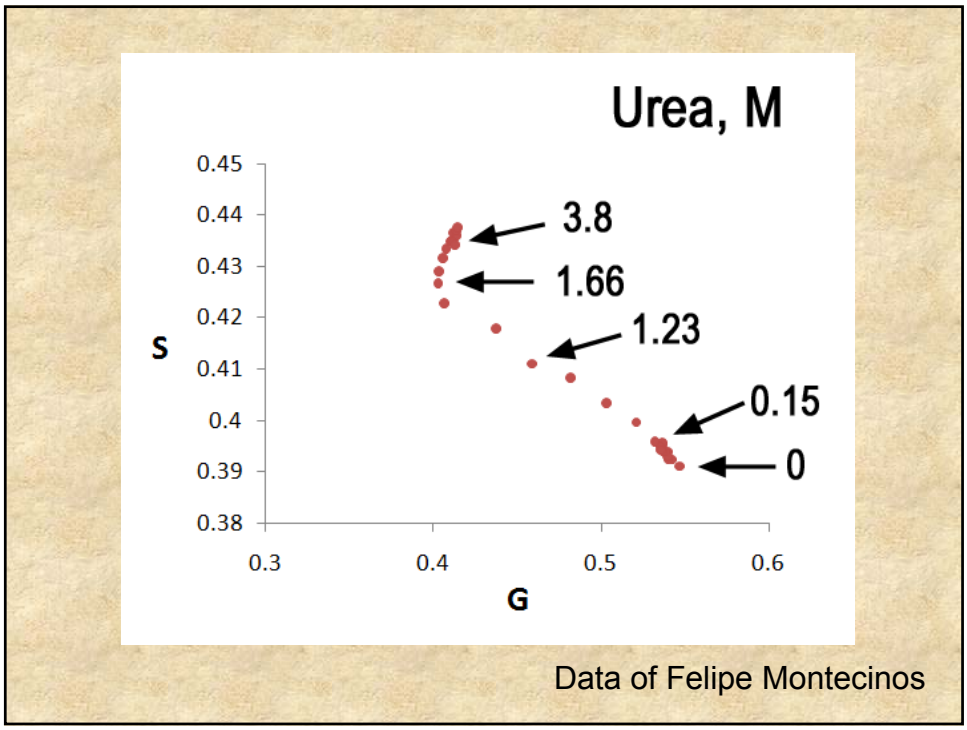

Data of Felipe Montecinos

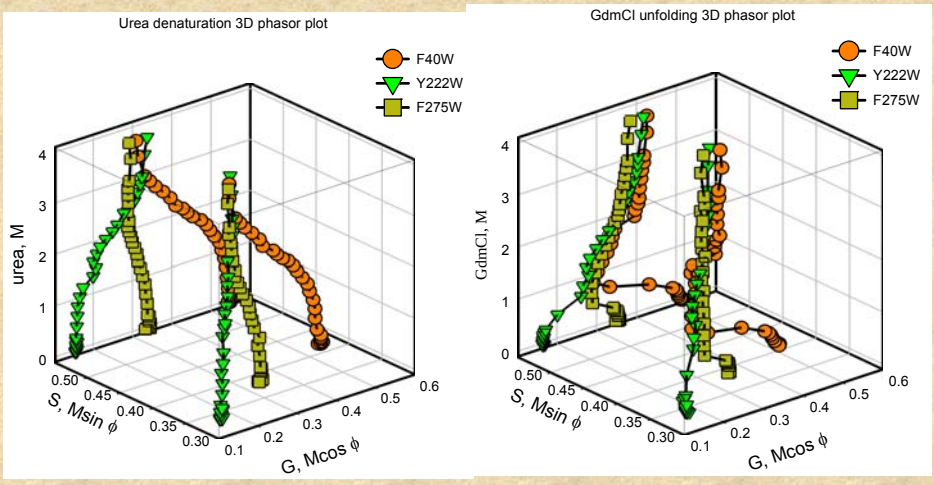

Montecinos-Franjola, F., James, N.G., Concha-Marambio, L., Brunet, J.E., Lagos, R., Monasterio, O., Jameson, D.M. (2014) Biochim Biophys Acta. 1844(7):1193-200. Single tyrptophan mutants of FtsZ: Nucleotide binding/exchange and conformational transitions.

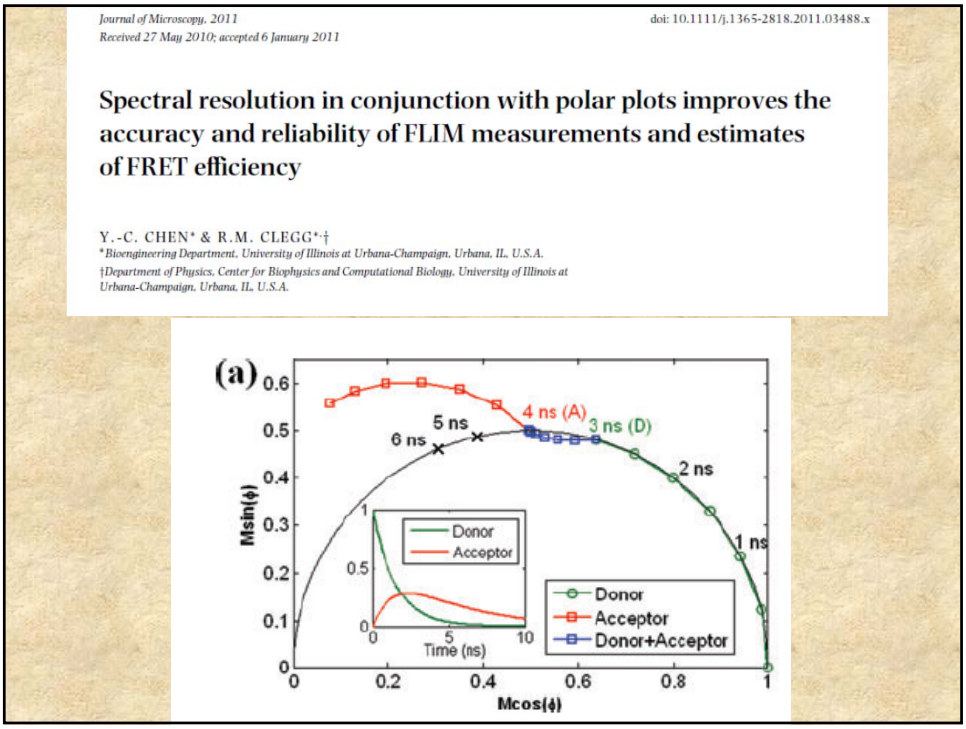
Journal of Microscopy, 2011
Received 27 May 2010; accepted 6 January 2011
doi: 10.1111/j.1365-2818.2011.03488.x

Spectral resolution in conjunction with polar plots improves the accuracy and reliability of FLIM measurements and estimates of FRET efficiency

Y.-C. CHEN* & R.M. CLEGG*†
*Bioengineering Department, University of Illinois at Urbana-Champaign, Urbana, IL, U.S.A.
†Department of Physics, Center for Biophysics and Computational Biology, University of Illinois at Urbana-Champaign, Urbana, IL, U.S.A.

FRET in GFP

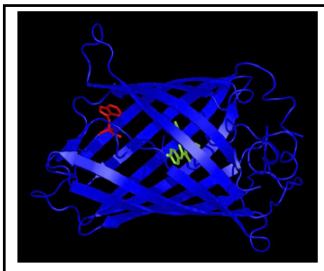

Fig. 1. 3D structure of GFP (blue) with the tryptophan in red and the fluorophore in green. (For interpretation of the references to colour in this figure legend, the reader is referred to the web version of this article.)

Direct observation of resonance tryptophan-to-chromophore energy transfer in visible fluorescent proteins

Nina V. Visser[a,d], Jan Willem Borst[a,b], Mark A. Hink[a,b], Arie van Hoek[a,c], Antonie J.W.G. Visser[a,b,e,*]

Biophysical Chemistry 116 (2005) 207 – 212

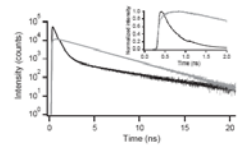

Fig. 3. Experimental (dotted line) and fitted (solid line) fluorescence decay curves of the tryptophan residue (black) and the fluorophore (gray) in green fluorescent protein. The excitation wavelength for both fluorophores was 300 nm. The detection wavelength for Trp fluorescence was 348.8 nm and for the fluorophore at wavelengths longer than 470 nm. The recovered parameters (α_i,τ_i) are collected in Table 1. The inset shows an enlarged view of the traces between 0 and 2 ns.

Table 1
Fluorescence decay parameters of tryptophan and fluorophore in visible fluorescent proteins upon excitation at 300 nm

Monitoring	α_1 (−)	τ_1 (ns)	α_2 (−)	τ_2 (ns)	α_3 (−)	τ_3 (ns)
Trp in EGFP	0.986	0.307 (0.295–0.308)	0.014	4.5 (4.3–4.6)	n.a.	n.a.
EGFP	−0.277	0.307 (0.295–0.308)	1.0	3.09 (3.09–3.10)	n.a.	n.a.
Trp in EYFP	0.999	0.240 (0.239–0.241)	0.001	5.3 (4.4–6.6)	n.a.	n.a.
EYFP	−0.243	0.240 (0.239–0.241)	1.0	3.81 (3.80–3.84)	n.a.	n.a.
Trp in ECFP	0.999	0.206 (0.206–0.209)	0.001	6.3 (5.4–7.9)	n.a.	n.a.
ECFP	−0.163	0.206 (0.206–0.209)	0.368	1.20 (0.93–1.48)	0.632	3.81 (3.72–3.93)

Values in parentheses are the confidence limits obtained after a rigorous error analysis at the 67% confidence level.
n.a. not applicable.

Table 2
Fluorescence (α_i, τ_i) and anisotropy (β_i, ϕ_i) decay parameters of the fluorophore in visible fluorescent proteins (VFP) upon excitation at 300 nm recovered after associated analysis

VFP	α_1 (−)	τ_1 (ns)	β_1 (−)	ϕ_1 (ns)	α_2 (−)	τ_2 (ns)	β_2 (−)	ϕ_2 (ns)	α_3 (−)	τ_3 (ns)
EGFP	−0.26	0.23 (0.19–0.25)	0.095 (0.092–0.097)	0.23 (0.22–0.24)	1.0	3.13 (3.11–3.15)	0.031 (0.030–0.032)	6.5 (6.0–7.0)	n.a.	n.a.
EYFP	−0.25	0.22 (0.19–0.26)	0.082 (0.079–0.085)	0.21 (0.20–0.23)	1.0	3.81 (3.77–3.82)	0.047 (0.046–0.048)	9.2 (8.8–9.7)	n.a.	n.a.
ECFP	−0.19	0.14 (0.09–0.19)	0.054 (n.f.–0.076)	0.22 (0.05–0.33)	0.36	1.26 (1.12–1.38)	0.028 (0.022–0.031)	13.9 (8.2–n.f.)	0.64	3.81 (3.74–3.84)

Values in parentheses are the confidence limits obtained after a rigorous error analysis at the 67% confidence level.
n.a. not applicable; n.f. not found.
In case of ECFP the contribution of ϕ_3 associated with τ_3 was very small.

FRET in GFP

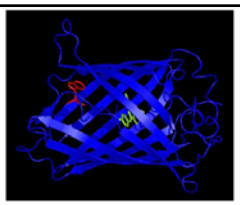

Fig. 1. 3D structure of GFP (blue) with the tryptophan in red and the fluorophore in green. (For interpretation of the references to colour in this figure legend, the reader is referred to the web version of this article.)

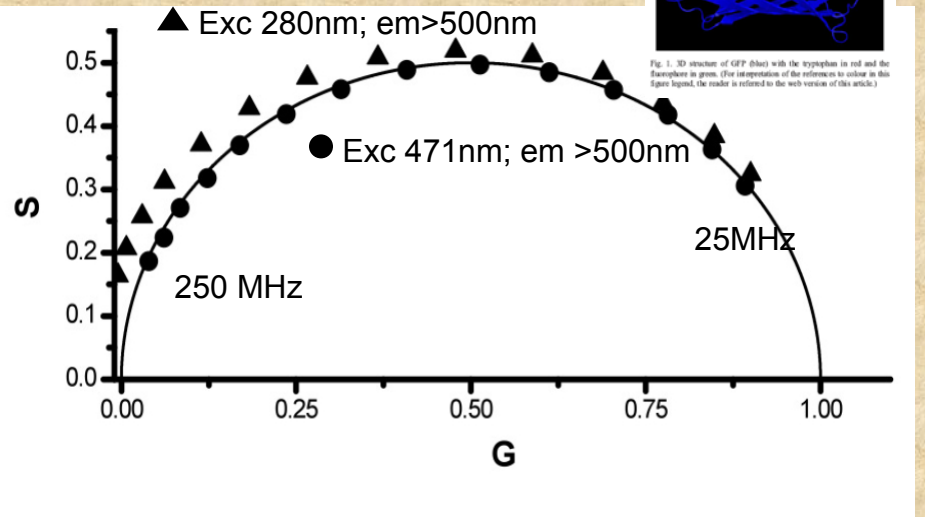

Enrico Gratton's phasor approach (implemented in the SimFCS software) plots a phasor point for each pixel in the image

Figure 5: FD FLIM data representation of the FRET standard.

From

Investigating protein-protein interactions in living cells using fluorescence lifetime imaging microscopy

Yuansheng Sun, Richard N Day & Ammasi Periasamy

Nature Protocols **6**, 1324–1340 (2011) doi:10.1038/nprot.2011.364

Published online 11 August 2011

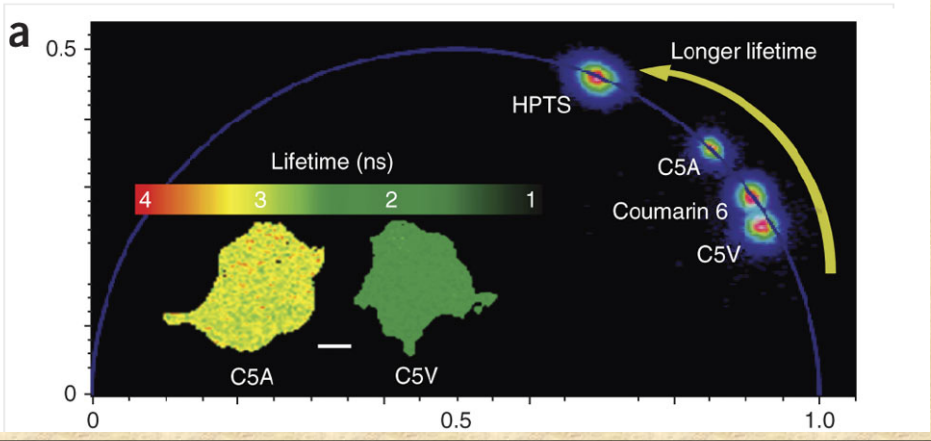

Separating Different Single exponential lifetimes using the ISS Fast FLIM system

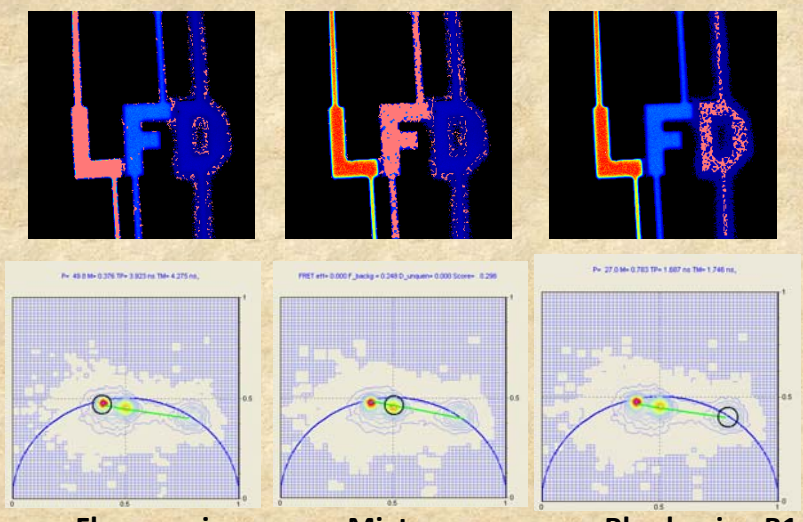

Pax-eGFP CHO-k1 in collagen

referenced with Fluorescein @ 905nm

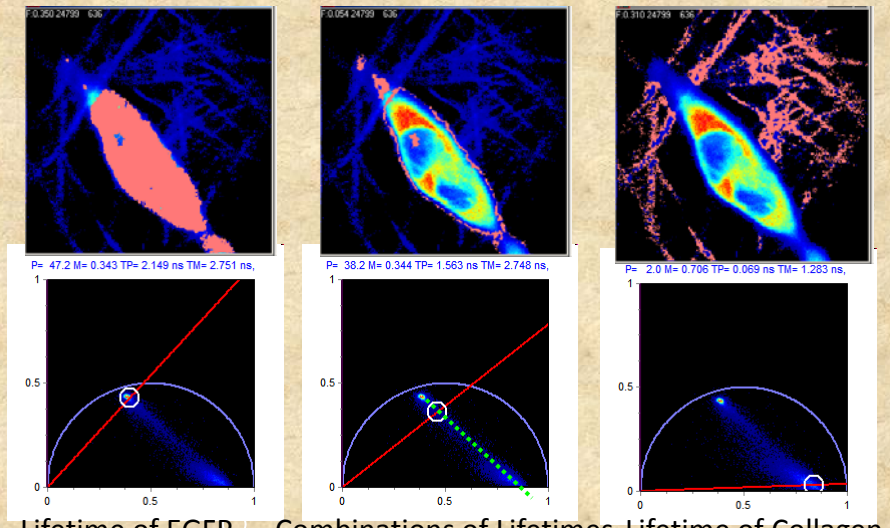

Lifetime of EGFP Combinations of Lifetimes Lifetime of Collagen

How to identify processes?

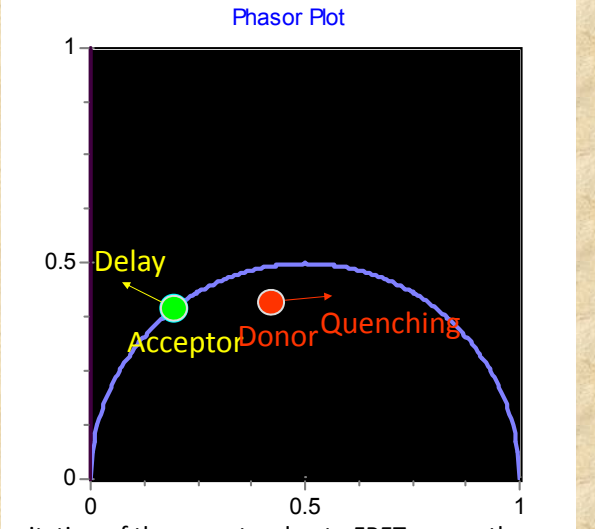

Delay of the excitation of the acceptor due to FRET moves the acceptor phasor to the left (yellow arrow). If the delay is sufficiently long, the phasor could fall outside the semicircle. The donor phasor moves to the right (red arrow) due to quenching (shorter lifetime).

If we have a donor with a single exponential decay that is quenched by the presence of a acceptor. What should we expect?

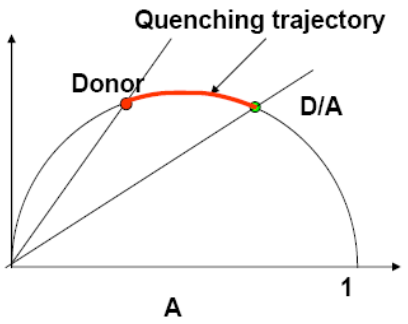

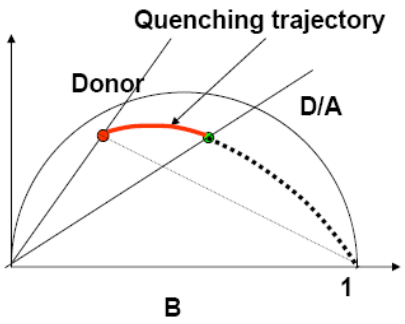

The lifetime of the donor is quenched
The FRET efficiency can be calculated by the ratio of the two lifetimes

If the donor lifetime is heterogeneous the phasor point will be inside the universal circle

- Can we quench up to zero lifetime?
- Even if we quench all the DONOR, we still are left with the autofluorescence.
- The final point is not at zero but at the autofluorescence phasor!!!

After all the Donor is quenched, what is left? The cell autofluorescence!!

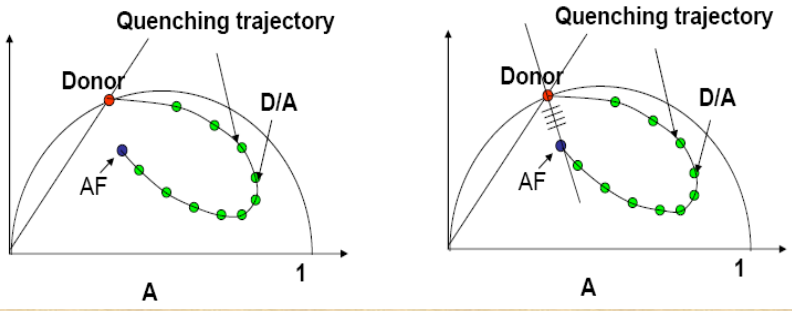

As the lifetime of the Donor is quenched, the phasor of the quenched Donor is added to the phasor of the autofluorescence

If there is a fraction of Donor that cannot be quenched, the final point will be along the line joining the Donor with the autofluorescence phasor

The pitfall of "conventional" FLIM analysis

Image obtained using B&H 830 in a 2-photon microscope

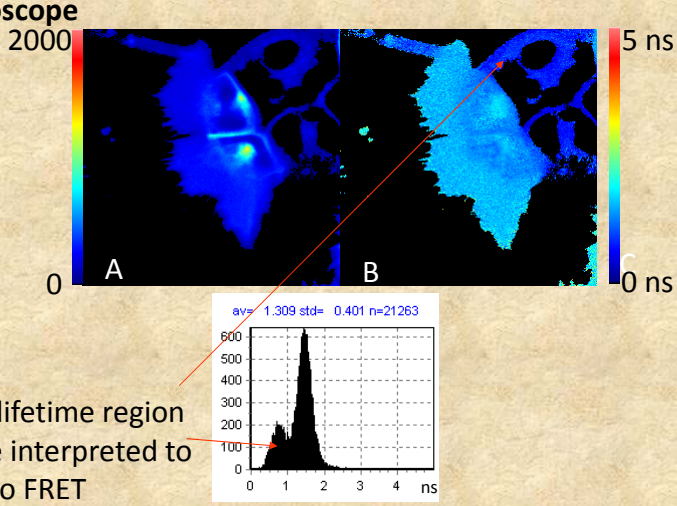

Shorter lifetime region could be interpreted to be due to FRET

Donor+acceptor+ligand. A) intensity image after background subtraction, B) τ_p image

Identification of FRET using the phasor plot

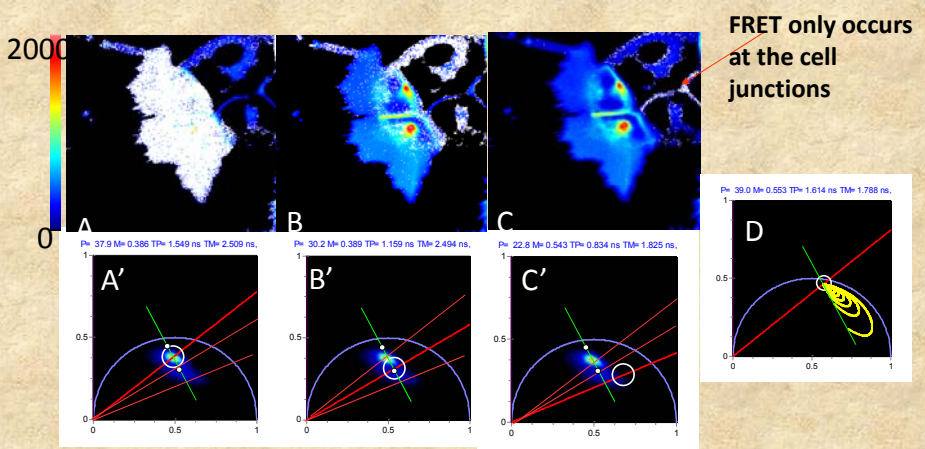

Selecting regions of the phasor diagram. Selecting the region in **A'** (donor +acceptor) the part in white lights up (**A**). Selecting the region in **B'** (autofluorescence) the part in white in lights up (**B**). The color scale in **B'** has been changed to better show the region of the autofluorescence. Selecting the region in **C'** (along the donor quenching line as shown in **D**) the part in white in at the cell junction lights up in **C**.

Phasor approach to fluorescence lifetime microscopy distinguishes different metabolic states of germ cells in a live tissue

13582–13587 | PNAS | August 16, 2011 | vol. 108 | no. 33

Chiara Stringari[a], Amanda Cinquin[b,c], Olivier Cinquin[b,c], Michelle A. Digman[a], Peter J. Donovan[b,d], and Enrico Gratton[a,1]

[a]Laboratory of Fluorescence Dynamics, Biomedical Engineering Department, [b]Department of Developmental and Cell Biology, [c]Center for Complex Biological Systems, and [d]Department of Biological Chemistry and the Sue and Bill Gross Stem Cell Research Center, University of California, Irvine, CA 92697

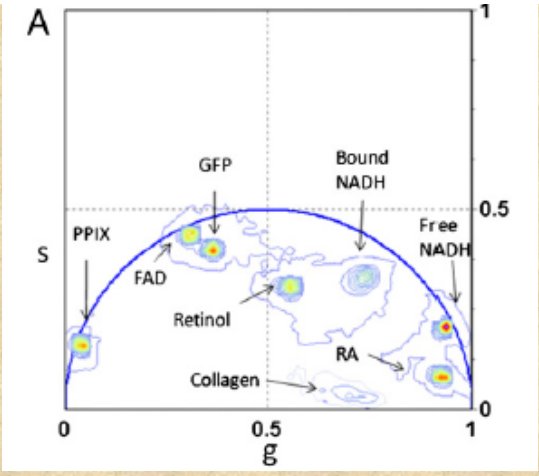

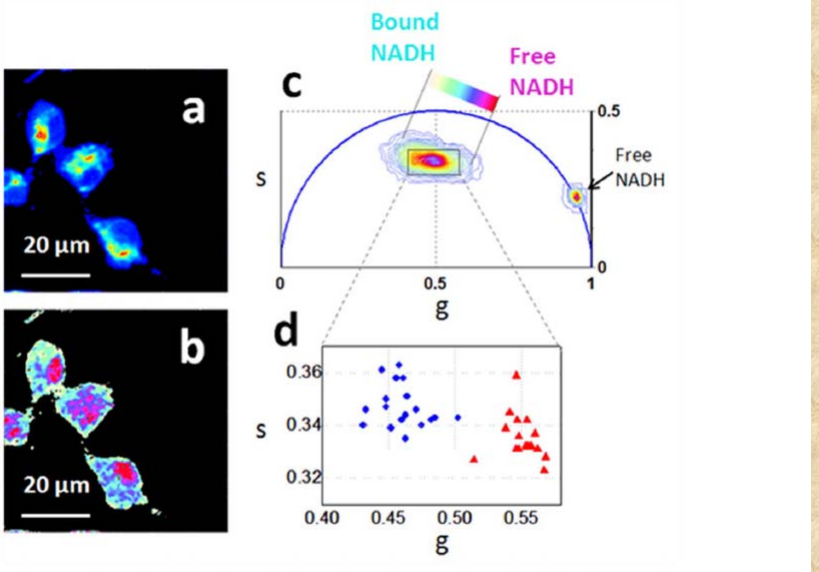

Figure 1. Free and bound NADH distribution within NPSCs. Two-photon fluorescence intensity images (a) and free/bound NADH FLIM maps (b) of the E12 NPSCs excited at 740 nm (c) FLIM phasor plot of E12 NPSCs autofluorescence. A linear cluster represents relative concentrations of free NADH (purple) and bound NADH (cyan-white). Red-purple color indicates a high free/bound NADH ratio, while violet, cyan and white indicate linearly and progressively decreasing ratios of free/bound NADH. (d) Scatter plot of the cell mitochondria (blue circle) and cell nuclei (red triangles). Nuclei contain a higher concentration of free NADH, while mitochondria contain mainly bound NADH.
doi:10.1371/journal.pone.0048014.g001

That's all!!!